Pervasive Under-Dominance in Gene Expression Underlying Emergent Growth Trajectories in *Arabidopsis thaliana* Hybrids

Wei Yuan, Fiona Beitel, Thanvi Srikant, Ilja Bezrukov, Sabine Schäfer, Robin Kraft, Detlef Weigel*

Department of Molecular Biology, Max Planck Institute for Biology Tübingen, 72076 Tübingen, Germany

*Corresponding author. Email: weigel@tue.mpg.de

Complex traits, such as growth and fitness, are typically controlled by a very large number of variants, which can interact in both additive and non-additive fashion. In an attempt to gauge the relative importance of both types of genetic interactions, we have turned to hybrids, which provide a facile means for creating many novel allele combinations. We focused on the interaction between alleles of the same locus and performed a transcriptomic study involving 141 random crosses between different accessions of the plant model species *Arabidopsis thaliana*. Additivity is rare, consistently observed for only about 300 genes enriched for roles in stress response and cell death. Regulatory rare-allele burden affects the expression level of these genes but does not correlate with F_1 rosette size. Non-additive gene expression in F_1 hybrids is much more common, with the vast majority of genes (over 90%) being expressed below parental average. Unlike in the additive genes, regulatory rare-allele burden in the non-additive gene set is strongly correlated with F_1 rosette size, even though it only mildly covary with the expression level of these genes. Our study underscores under-dominance as the predominant gene action associated with emergence of rosette growth trajectories in the *A. thaliana* hybrid model. Our work lays the foundation for understanding molecular mechanisms and evolutionary forces that lead to dominance complementation of rare regulatory alleles.

Introduction

When expression and inheritance of a trait is under control of many genes, it is considered a quantitative or complex trait, with growth- and fitness-related traits being almost always complex traits (Braendle et al. 2011; Falconer and Mackay 1996). The complexity of these traits comes not only from the large number of underlying genes/loci, but also from the multitude of potential allelic interactions within and between the genes involved. The best-understood type of allelic interaction is the additive effect, in which different alleles contribute to a trait co-dominantly, and the offspring have an intermediate trait value that is close to the average of the two parental alleles. By definition, non-additive genetic effects are any deviations from this additive scenario, with two common examples being dominance and epistasis (Falconer and Mackay 1996). Due to limitations in technical and statistical frameworks, non-additive effects are much less studied and understood than additive effects (Varona et al. 2018). Nevertheless, there is evidence that non-additive effects can be pervasive and contribute substantially to what had for some time been perceived as "missing-heritability" (Mackay et al. 2009; Zuk et al. 2012; Hemani et al. 2013). Additive and non-additive genetic effects are best revealed in heterozygotes, in which contributions of different alleles to a phenotype of interest can be easily partitioned.

Causal genetic variants often exert their functional effects by modulating gene expression. Measuring gene expression differences and associating the variation with complex traits provides information regarding biological functions and processes causing natural phenotypic variation (Albert and Kruglyak 2015). Over the last decade, statistical frameworks such as Transcriptome-wide association (TWA) and expression QTL (eQTL) have rapidly matured, providing insights into molecular functions of complex traits (Albert and Kruglyak 2015; Wainberg et al. 2019). The highly quantitative nature of transcriptomic, especially RNA-seq data provides an excellent opportunity for tracking additive versus non-additive gene actions. By comparing the expression level of a gene in F_1 heterozygotes to that of the parental average, one can easily calculate the degree of its non-additivity (Jeffrey Chen 2013).

51 Above-ground biomass accumulation is a fitness-related trait that has important bearing on
52 both local adaptation of wild plants (Vogel et al. 2019) and performance of agricultural species
53 (Batts et al. 1997; Elings et al. 1997). In the inbreeding plant *Arabidopsis thaliana,* rosette-size, a
54 close proxy for above-ground biomass, is not only a primary indicator of growth and general
55 performance (Julkowska et al. 2016; González et al. 2020), but also both highly variable (González
56 et al. 2020; Wieters et al. 2021) and strongly associated with fitness (Korves et al. 2007; Wieters et
57 al. 2021). The range of variation in this trait can be substantially increased by including F_1 hybrids.
58 While rare combinations are smaller than any naturally occurring accession (Bomblies and Weigel
59 2007; Chae et al. 2014), most F_1 hybrids have larger rosettes (Seymour et al. 2016; Yang et al. 2017;
60 Oakley et al. 2019), an emergent positive phenotype that in outbreeding crops is usually termed
61 heterosis. F_1 hybrids are a particularly interesting systems to study, as alleles that are naturally
62 segregated into different genomes are brought into contact with each other, leading to numerous
63 novel genetic interactions (Landry et al. 2007; Rieseberg et al. 2007). It has long been postulated
64 that these novel genetic interactions, both additive and non-additive, may contribute to hybrid
65 performance (Birchler et al. 2003; Rieseberg et al. 2007; Bell et al. 2013).

66 We are interested in understanding how common additive and non-additive gene action is,
67 and how it relates, if at all, to growth phenotypes in F_1 hybrids. Specifically, we would like to learn
68 at the species level (i) whether additive and non-additive gene actions occur at similar frequency,
69 (ii) whether the gene actions are mostly specific to parental combinations, or if certain genes and
70 pathways particularly frequently exhibit one of the effects, (iii) and whether emergent phenotypes
71 in F_1 hybrids are more likely to result from additive or non-additive gene actions. *Arabidopsis*
72 *thaliana* provides a powerful system to address these questions, due to the wealth of genomic
73 resources and large collection of natural accessions (1001 Genomes Consortium). Previous studies
74 of intra-specific *A. thalian* hybrids have provided insights into mechanisms affecting hybrid
75 performance, such as the mitigation of defense-growth tradeoffs in superior hybrids (Miller et al.
76 2015), and on the flip side, greatly compromised growth in hybrids due to incompatible allelic
77 interaction and excessive activation of defense (Chae et al. 2014).

We designed a study in *A. thaliana* that surveyed not only a broad range of the species' genetic diversity, but also allowed for the detection of interactions between an exceptionally large number of alleles. We find non-additivity in gene expression in F_1 hybrids to be common, with non-additive genes being much more commonly expressed below the parental average (mid-parent value, MPV) than above it. Expression close to the MPV in turn is rare, with a substantial fraction of such genes having a role in biotic defense pathways, suggesting that defense is particularly well buffered.

Results

Non-additive gene action is more abundant in F_1 hybrids

For our work, we drew on resources from the 1001 Genomes Project for this species (1001 Genomes Consortium), crossing resequenced, naturally inbred accessions to generate a panel of F_1 hybrids. To broadly survey possible genetic interactions, and to evaluate whether consistent patterns of additive and non-additive gene expression exist, we carried out an RNA-seq experiment for which 101 parent-F_1 trios, *i.e.*, each F_1 hybrid and their inbred parents, were planted (Fig. 1A, Data S1, Methods). Of all genotypes, 82 F_1s and 124 inbred parents were included in the final analyses. Whole-rosette sizes, a good proxy for biomass (Fig. S1, Methods), were measured in inbreds and F_1s.

The expression of many genes changes in F_1 hybrids relative to the parents (Jeffrey Chen 2013). Under an additive model, gene expression in F_1 hybrids is close to the parental average. We asked whether there are genes that are almost always additively, or non-additively expressed in F_1s across all trios. We identified close to 900 genes that were consistently expressed in an additive fashion (Fig. S2, Methods), and 1,805 genes (Data S2) that were consistently expressed non-additively (Fig. S3, Methods) in all trios. Both the additive and the non-additive genes had distribution profiles of transcript abundances and coefficients of variation that were similar to background genes (Fig.1C-D), *i.e.*, including both high- and low-abundance transcripts as well as

103 ones that varied little across samples or ones that varied substantially. This indicates that expression
104 level and variance did not greatly bias our ability to discover specific gene expression patterns.
105 Parenthetically, the great majority of the additive genes had very low ranks on their non-additive
106 score (Fig. 1E), confirming that our gene calling algorithm successfully selected for contrasting gene
107 actions. Within our non-additive genes, only 150 (~8%) of these were consistently expressed above
108 MPV in the F_1s. For the great majority of genes, low expression level was dominant, such that most
109 genes were expressed in the F_1s at a level between the lower parent and the MPV.

110 Gene Ontology (GO) term analysis revealed that the additive genes are strongly enriched
111 in cell death- and stress response-related processes (Fig. 1B). Because expression level close to
112 parental average would be indicative of canalization, our result suggests that the cell death- and
113 stress-response pathways are systematically buffered in F_1s. In comparison, non-additive genes are
114 featured in much more diverse biological processes (Fig. 1G), including regulation of immune
115 system process, ribosomal RNA transcription, plant organ formation, and others.

116 Non-additive gene expression is thus pervasive in F_1 hybrids, with the overwhelming
117 majority of genes expressed below the parental average. Many biological processes are affected in
118 the F_1s by non-additive expression, as the GO enrichment suggested.

119 Non-additive genes covary with size

120 We reduced the dimensionality of our non-additive gene set by grouping genes with a similar
121 behavior across samples via k-means clustering (k=13). We examined how well the behavior of
122 different clusters across samples was correlated (Fig. 1F), finding that one particular cluster (cluster
123 6, n=116) behaved in a manner that was opposite to that of all other clusters.

124 Probing into the underlying commonalities between the genes that drove the clustering, we
125 discovered that mean expression value for eight of the clusters (clusters 6-13) covaried with rosette
126 size in both inbreds and hybrids. The most distinct cluster 6 showed a clear positive correlation,
127 while the other clusters were negatively correlated with rosette size (Fig. 2A). While the general

128 trend of correlation between gene expression and rosette size remained the same in F_1s and the
129 inbred parental lines, the shape of the correlation differed.
130

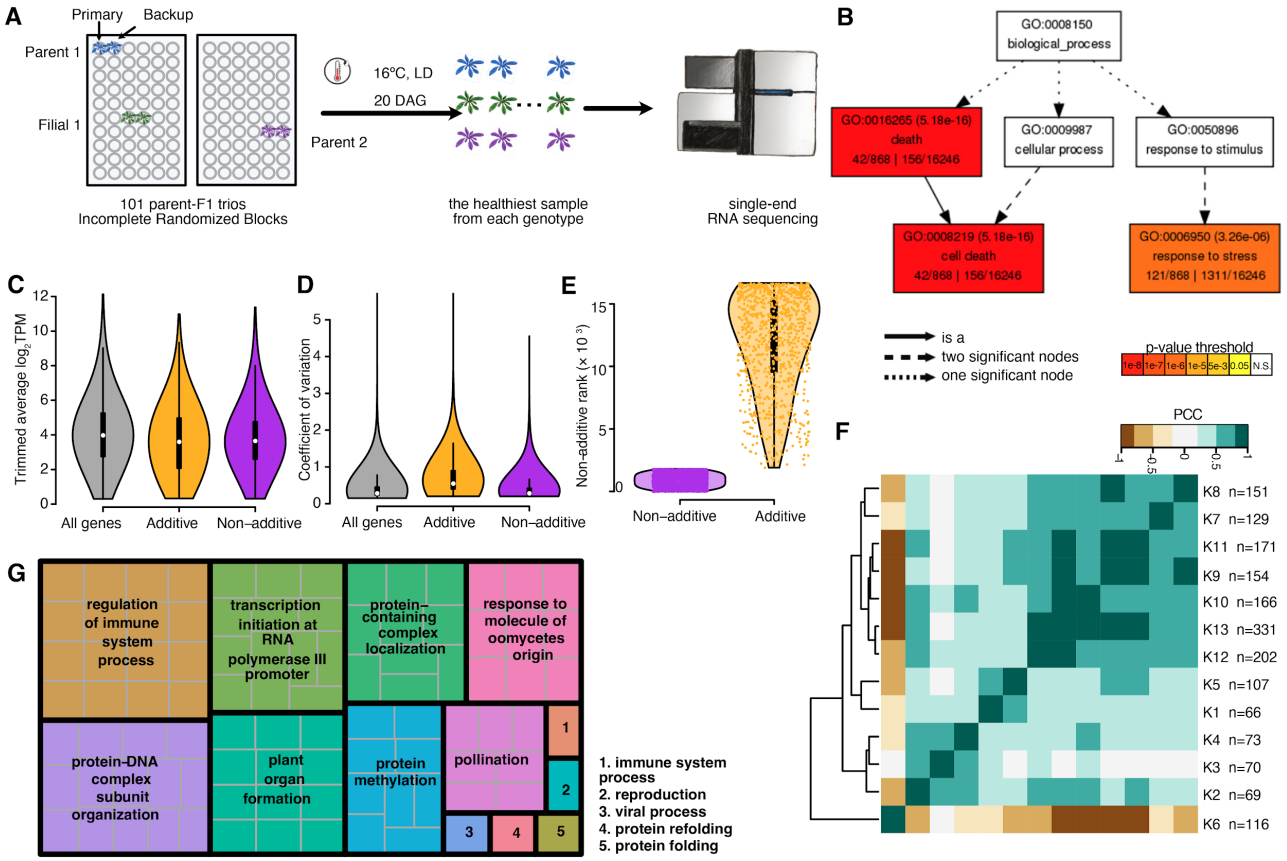

131

132 **Figure 1. Summary of additive and non-additive genes. A.** Experimental set-up. Note that not all trios were
133 completely sequenced and analyzed. **B.** GO-term (biological process) enrichment of additive genes. **C-D.**
134 Both additive and non-additive genes showed average transcript abundance (C) and coefficient of variation
135 (D) profiles comparable to those of all genes in the background. **E.** Additive genes ranked low by their non-
136 additive score. **F.** Correlation among all non-additive gene clusters. Pearson correlation coefficients were
137 calculated using cluster average. **G.** Revigo summary of biological processes enriched in non-additive genes.
138

139 To obtain further insight into the above observations, we formally investigated the
140 relationship between average gene expression of each cluster and rosette size, by performing
141 Bayesian linear-mixed-model spline fitting (Fig. 2B, Fig. S4, Methods). Clusters 1-5 showed no clear
142 trend of association between expression and size, cluster 6 showed expression increasing in parallel
143 with rosette size (Fig. 2B, top panel), and the remaining clusters showed expression decreasing with

144 increasing rosette size. For these seven clusters, F_1 hybrids tended to have lower expression than
145 the inbreds across the entire range of rosette size (Fig. 2B, bottom panel). GO analysis did not
146 indicate that clusters were specific for particular biological processes.

147 Therefore, a large number (n=1,420) of non-additively expressed genes showed covariation
148 of expression level with rosette size. F_1 hybrids systematically exhibited a shift towards either lower
149 or higher expression levels in the direction consistent with the change in rosette size relative to
150 inbred parental lines. The trend is unique for non-additive genes, as repetitive random subsets of
151 the transcriptome showed neither profound covariation with size nor a systematic shift in the
152 expression level in F_1s (Fig. 2C-D).

153 F_1 exhibits robust growth advantage

154 That gene expression exhibited a systematic shift in the F_1 hybrids, and that non-additive gene
155 expression in the F_1s covaried with rosette size prompted us to ask (i) whether degree of non-
156 additive expression within individual parent-hybrid trios correlated with rosette size differences
157 between the F_1s and their parents, and (ii) whether a global perturbation to the plant's
158 developmental program would affect the F_1s and the inbreds differently. To this end we conducted
159 a second experiment in which we applied BTH (acibenzolar-S-methyl), an analog of the defense
160 hormone salicylic acid (SA) (Fig. 3A, Methods), to 40 parent-F_1 trios. Induction of pathogen defense
161 was chosen as treatment because it causes morphological changes and at least sometimes
162 extensive transcriptional reprogramming, as has been observed in some F_1 hybrids of *A. thaliana*
163 *(Bomblies et al. 2007)*.

164 F_1 hybrids are on average considerably larger than the inbred parents (inbred mock:
165 118.2±61.1 mm^2, F_1 mock: 157.1±79.6 mm^2, inbred BTH: 71.6±35.5 mm^2, F_1 BTH: 94,3±44.3 mm^2,
166 Fig. 3B), consistent with our earlier experiment (Fig. S5). Neither the distribution of the rosettes of
167 the parents nor those of the F_1 plants was normal, with the F_1 population having a significantly
168 higher number of larger individuals (p=8e-5, two-tailed Kolmogorov-Smirnov).

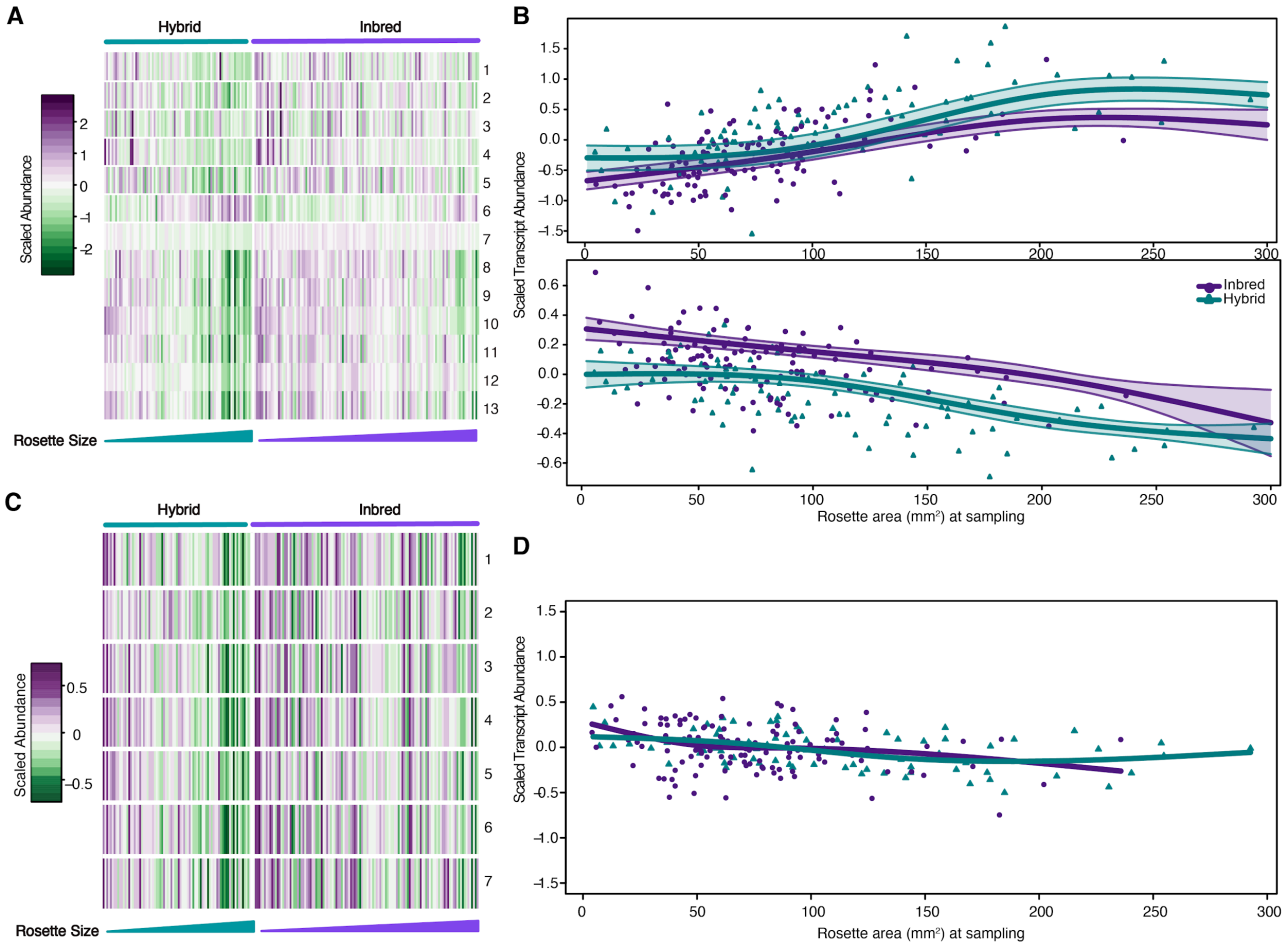

Figure 2. Non-additive gene expression level correlates with final rosette size. A. Heatmap showing the average expression of each non-additive gene cluster in each sample, sorted into F_1s and inbred parental lines, and arranged by ascending final rosette size. **B.** Linear-Mixed-Model spline fitting of exemplary clusters. Top: cluster 6, bottom: cluster 7; points: cluster mean expression in each sample; shaded area: 95% Bayesian credible intervals. **C.** Heatmap of the average expression of gene clusters from 500 randomly sampled genes, arranged in the same order as in Fig. 2A. **D.** Randomly sampled genes, which show little expression-size covariation and no differences between inbreds and F_1s.

In a comparison of randomly chosen trios, the F_1 was almost twice as likely as one of the inbreds to be the larger individual (Cliff's delta=0.31). BTH treatment significantly reduced plant size in both inbreds and hybrids (mock: 79.2±3.0 mm^2, BTH: 39.5±4.2 mm^2, One-way ANOVA, $p<2x10^{-16}$, Fig. 3B, D, Fig. S6), and induced considerable variation in growth responses (Fig. 3E, Fig. S7). F_1s exhibited stronger size reduction but remained to be more likely to be larger than either parent (p=0.0002, two-tailed Kolmogorov-Smirnov, Cliff's delta=0.31). Most trios showed similar patterns

184 in rosette size growth emergence after both mock- and BTH-treatment, with the majority of F_1s
185 remaining larger than the MPV (Fig. 3C).
186

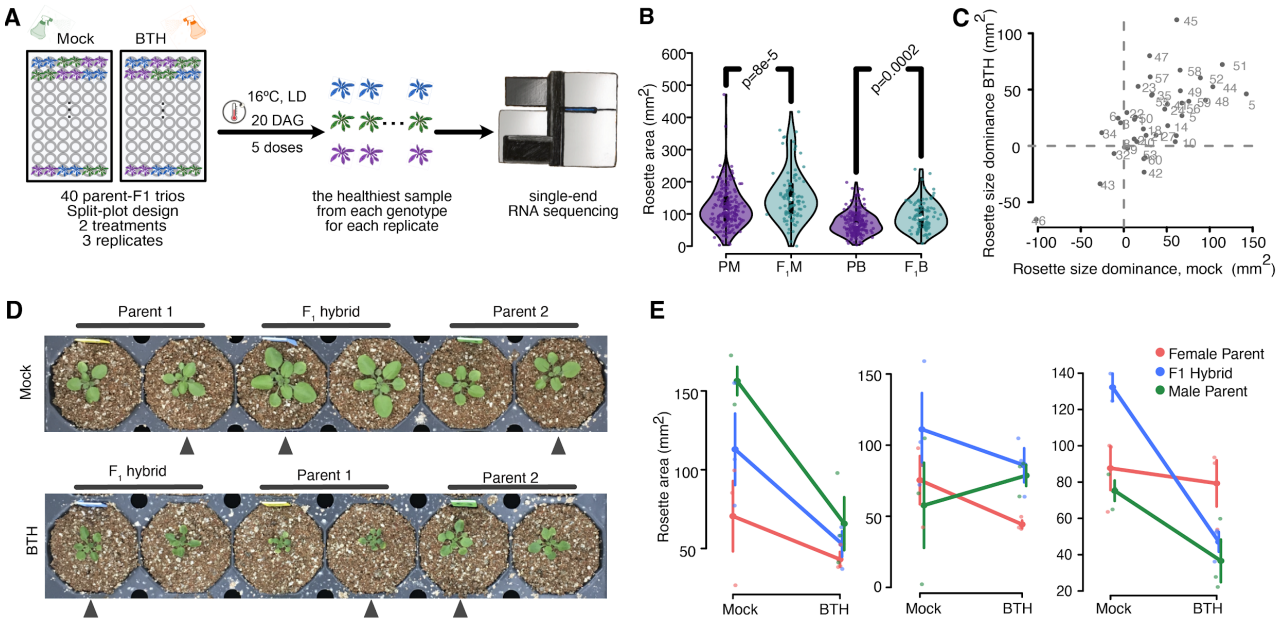

187

188 **Figure 3. BTH treatment reduced rosette size in both inbreds and F_1s. A.** Experimental design. **B.** F_1s
189 maintained robust growth advantage despite the reduction in rosette size upon BTH treatment. PM: parent
190 mock, F_1M: F_1 hybrid mock, PB: parent BTH treated, F_1B: F_1 BTH treated. **C.** Positive correlation between
191 rosette size dominance under mock and BTH conditions. Numbered labels indicate the ID of the SHB2 trios.
192 **D.** Typical rosette phenotype of a trio. **E.** Diverse response of three example trios to BTH treatment. Reaction
193 norm lines connect the mean ± SD rosette area of each genotype under both treatments.
194

195 Growth advantage is therefore prevalent in the F_1 hybrids included in both of our
196 experiments (Fig. 3B, Fig. S5), and is to a great extent robust to a perturbation of the developmental
197 program. Although we cannot rule out that even stronger BTH treatment would eventually render
198 hybrids smaller than the inbreds, it is, however, unlikely to occur in a natural setting, as our
199 treatment already resulted in extremely dwarfed plants.
200

201 **Degree of non-additivity correlates with F_1 growth advantage**

202 Having established that non-additively expressed genes are systematically associated with plant
203 size, and that F_1 rosettes frequently exhibit positive size emergence, we investigated whether the
204 degree of expression non-additivity in F_1s may be associated with this phenotypic non-additivity.
205 We focused on genes showing general response to BTH treatment (n=6,371) and asked whether
206 deviations of F_1 expression values from the MPV of any gene in individual trios exhibited correlation
207 to the non-additivity in F_1 rosette size. Clear correlations could be observed for many genes, which
208 could be broadly categorized into (monotonic) positive, (monotonic) negative, or quadratic (Fig.
209 4A), while in some cases no correlation was observed. We defined 61 groups of genes that fell into
210 these different categories by k-means clustering. To establish the significance of the size-expression
211 correlation, we performed a Wilcoxon signed-rank test on the genes in each of the 61 clusters (Fig.
212 4B, Methods, Data S3). Some clusters shared similar relationships between the non-additivity in
213 gene expression and rosette size, therefore we sorted the clusters further into 12 classes reflecting
214 the pattern of correlation under mock and BTH treatment (e.g., "negative-negative" means
215 negative correlation under both treatments, Fig. 4C, Methods). Correlation often changed in
216 response to treatment, with the majority of genes exhibiting negative correlation with rosette size
217 non-additivity under at least one condition, a trend that increased after BTH treatment (Fig. S8).
218 This observation is consistent with your finding that negative dominance is more pervasively
219 associated with rosette growth in *A. thaliana*.

220 The genes with negative size-expression correlation after BTH treatment (Data S4, "negative
221 genes" hereafter) are enriched for GO terms "regulation of gene expression", "floral organ
222 development", and "response to (abiotic) stimuli" (Fig. 4D, Fig. S9). Genes with positive correlation
223 under both treatments (Data S5 "positive genes" hereafter) were moderately enriched for
224 photosynthesis (Fig. S10). While it seems unlikely, we cannot exclude that the enrichment for abiotic
225 response is due to our analytic focus on BTH-responsive genes, although a parallel GO enrichment
226

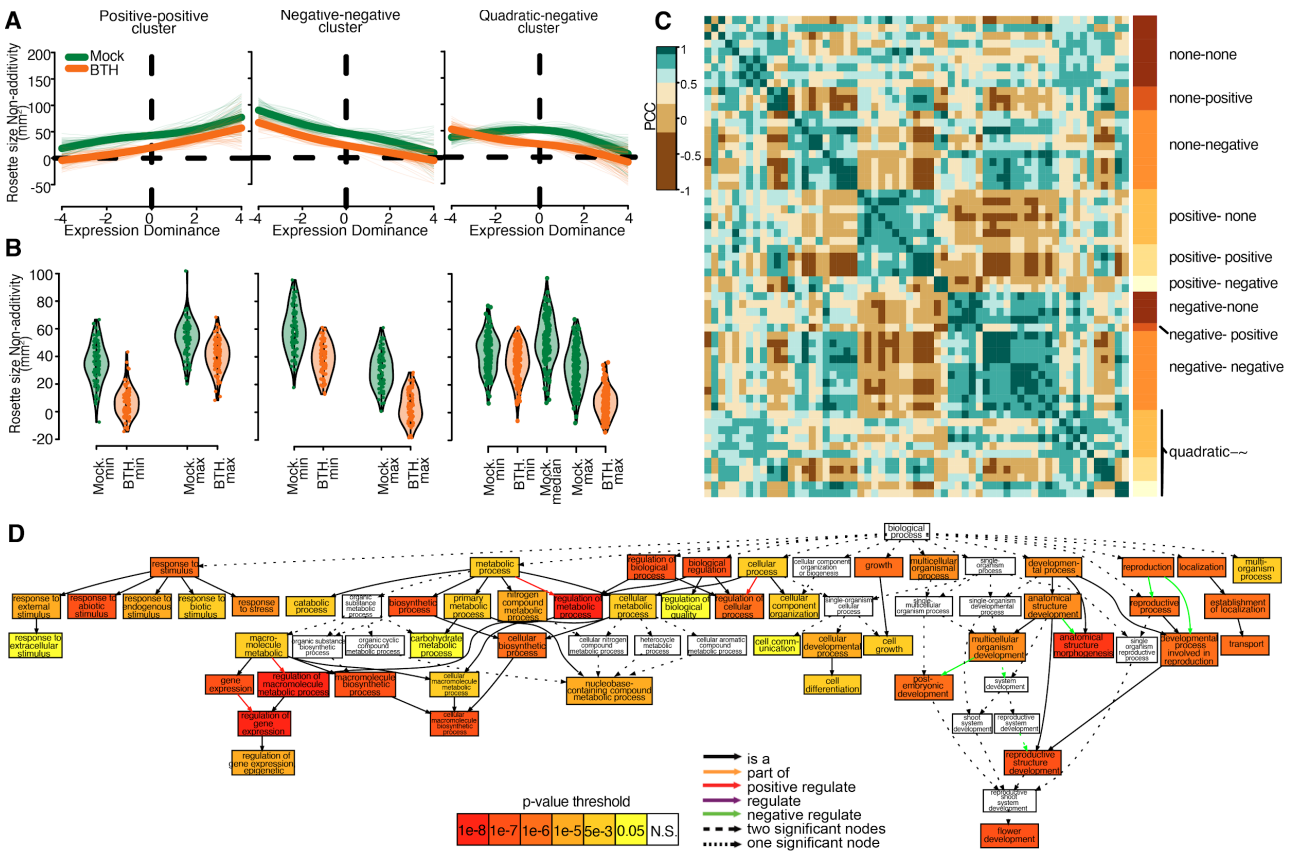

E

known motif search (Plant promoters) - top hits

	p-value	%Targets	Match	Gene group	No. Genes
	1e -42	26.65	PCF	All BTH negative	2248
	1e -13	24.89	PCF	Negative-negative	880
	1e -31	27.78	PCF	Only BTH negative	1368
	1e -13	28.86	PCF	Positive-positive	499

F

de novo motif search - top hits

	p-value	%Targets	Match	Gene group	No. Genes
	1e -54	28.16	PCF	All BTH negative	2248
	1e -18	17.05	PCF	Negative-negative	880
	1e -47	19.15	PCF	Only BTH negative	1368
	1e -19	24.85	PCF	Positive-positive	499

Figure 4. Genes whose degree of non-additive expression in trios correlates with hybrid performance. A. Exemplary clusters of "positive-positive" (left), "negative-negative" (middle), and "quadratic-negative" (right) genes. Thick solid line: spline fitting of the cluster means; thin lines: spline fitting of individual cluster members. **B.** Average biomass MPH for rosette samples with low- vs. high- expression of genes in the same clusters as in A. Each violin depicts the distribution of cluster gene expression averaged across the top and the bottom (and the middle for the quadratic relationship) deciles of samples. **C.** Pearson correlation coefficients (PCC) of all 61 clusters based on LMM-spline modeling. The clusters are further sorted into 12 classes labeled on the right according to the relationship between gene expression and biomass under mock or BTH treatment. **D.** GO enrichment for genes from the negative cluster; see Fig. S10 for more details. **E.** Regulatory regions of genes from both positive and negative clusters are enriched for a PCF binding motif. **F.** De novo motif search confirmed enrichment of the PCF motif.

240 test for all BTH-responsive genes did not return significant hits in any biological process. Together
241 these results suggest that the F_1 transcriptome is systematically repressed in reproductive growth
242 and (abiotic) stress response functions while activated in photosynthesis. Such non-additive
243 transcriptome signature is associated with the rosette growth advantage of the F_1s, which is
244 pervasive in our system.

245 To begin to discover potential regulatory mechanisms, we performed motif enrichment
246 analysis among the heterosis associated genes (Methods). PROLIFERATING CELL FACTOR (PCF)
247 and c-Myc transcription factor binding motifs are highly enriched in the promoters of negative
248 genes (569/2,248 genes, $p=10^{-42}$, and 433/2,248 genes, $p=10^{-21}$, Fig. 4E, Fig. S11). PCF-binding
249 motifs are also highly enriched in the positive genes (144/499 genes, $p=10^{-13}$, Fig. 4E). These
250 findings were corroborated by *de novo* motif searches (Fig. 4F). PCF/TCP proteins constitute a
251 conserved plant-specific transcription factor family that includes several regulators of cell cycle,
252 growth, and disease resistance (Gonzalez 2015; Li 2015). That both positive and negative genes
253 were enriched for PCF motifs points to these factors as a potential central toggle for global re-
254 modeling of hybrid transcriptomes.

255 Parenthetically, close to 900 additively expressed genes were called from the second
256 experiment, and 300 of which (hereafter, common additive genes) overlapped with the first
257 experiment (Fig. S12, Data S6, Methods). GO-term analysis of the common additive genes revealed
258 enrichment in cell death- and stress response-related processes (Fig. S12), again confirming that
259 these pathways are systematically buffered in F_1s. As expected, the additive genes from the second
260 experiment were more enriched for defense response than the genes from the first experiment
261 without BTH treatment (Fig. S13).

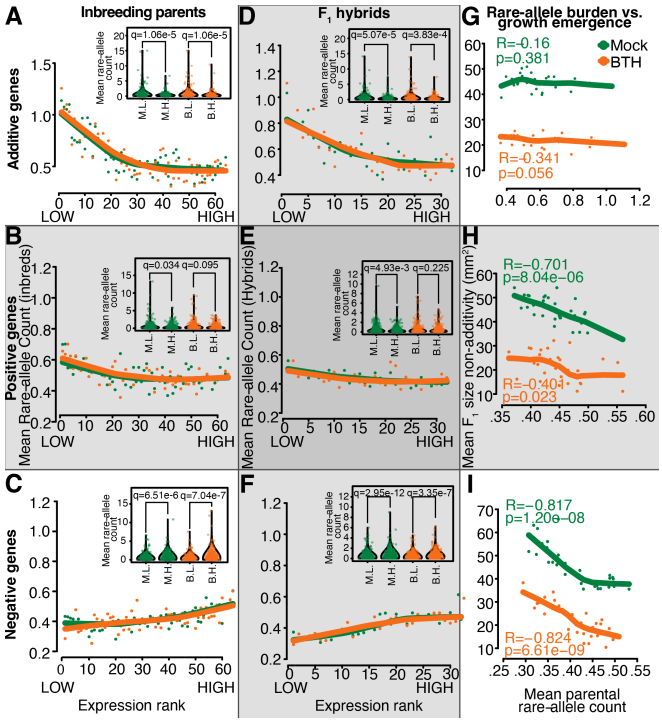

Figure 5. Rare allele burden affects gene expression and emergence of F_1 growth advantage. A-C. Association between gene expression rank and upstream rare allele count of additive genes (A), positive genes (B), and negative genes in inbred parents (C). Samples were ranked by expression value for every gene within the gene list. Points: average upstream rare allele counts of all samples sharing the same rank; lines: LOWESS trend lines. Insets show the upstream rare-allele count of samples in the top (Mock 10, BTH10) and bottom decile (Mock 1, BTH 1) of expression ranks. **D-F.** Association between gene expression rank and upstream rare allele count of three gene lists in F_1 hybrids. **G-I.** Association between rosette growth emergence and mean parental rare allele burden in additive (G), positive (H), and negative (I) genes. For each gene, F_1s were ranked by average number of rare alleles in their parents. Points: average non-additivity in rosette size of all F_1s sharing the same rank; lines: LOWESS trend lines

Dominant, not additive complementation underlies emergence of F_1 growth advantage

We next asked whether the association between expression level and F_1 growth has a common genetic basis. Hybrids offer a genomic playground where deleterious alleles from each of the parental genomes may be complemented, one of the leading hypotheses for growth advantage in hybrids. Deleterious alleles are expected to be segregating at lower frequency in the population, and those residing in the gene regulatory regions have been associated with mis-expression of genes in *cis* (Kremling et al. 2018). To gauge the effect of genetic complementation in the F_1s, we

turned to regulatory rare alleles, looking into the relationship between gene expression level and the average number of regulatory rare SNPs (within 1 kb upstream of genes), which are more likely to have a deleterious effect on gene expression than common SNPs, in both inbred parents and the F_1s (Methods).

Regardless of the treatment, we observed on average a significantly higher rare allele counts upstream of the common additive genes associated with low expression ranks in inbred parents (Fig. 5A, Wilcoxon signed rank-sum test with Benjamin-Hochberg FDR: mock, $\alpha=1.1\times10^{-5}$, BTH: $\alpha=1.1\times10^{-5}$). The trend was moderate in the positive genes (Fig. 5B, mock: $\alpha=0.03$, BTH: $\alpha=0.10$) and in the opposite direction in the negative genes (Fig. 5C, mock: $\alpha=7\times10^{-6}$, BTH: $\alpha=7\times10^{-7}$). Trends in F_1s were in all three gene groups consistent with what was seen in the parents (Fig. 5D-F, $\alpha=5.1\times10^{-5}$, additive-mock; $\alpha=3.8\times10^{-4}$, additive-BTH; $\alpha=0.005$, positive-mock; $\alpha=0.23$, positive BTH; $\alpha=3\times10^{-12}$, negative-mock; $\alpha=3\times10^{-7}$, negative-BTH). Note that for the non-additive genes, increased upstream rare-allele count was always associated with an expression pattern that is consistent with a smaller plant. Upstream rare-allele burden therefore tends to lead to more extreme, and deleterious expression of these genes, in parents and the hybrids alike.

We next asked what the likely phenotypic consequence of the upstream rare-allele burden might be. Because non-additive gene expression varied less with rare-allele burden than additive gene expression (Fig. 5A, D), we expected these additive genes to be critical for F_1 growth advantage. To our surprise, the number of rare alleles upstream of these common additive genes did not seem to be particularly relevant for rosette growth advantage in the F_1s (Fig. 5G, Pearson correlation R=-0.16, p=0.38). Additive complementation may therefore be an inherent property of hybrids without directly influencing growth advantage. In contrast, the number of mean upstream rare alleles in both positive (Pearson correlation R=-0.701, p=8.04e-6) and negative (Pearson correlation R=-0.817, p=1.20e-8) genes is a strong negative predictor of rosette growth advantage in F_1 hybrids (Fig. 5H-I, suggesting that growth advantage tends to be greater in hybrids derived from parents with fewer rare alleles in the upstream regions of these non-additively expressed

genes. We conclude that dominant complementation contributes heavily to the F_1 growth advantage observed in our system.

Discussion

Most, if not all, of the growth and survival phenotypes of an organism are complex traits. Although the infinitesimal model predicts that non-additive effects contribute only minimally to most structural traits (Crow 2010), their impact is expected to be far greater in fitness-related traits (Merilä and Sheldon 1999). To date most of the methods for mapping and genomic selection are based on additive effects only (Varona et al. 2018). However, incorporating non-additive, *i.e.*,, dominant and epistatic, effects into quantitative genetics modeling can improve heritability estimates and accuracy of genomic prediction (Su et al. 2012; Wellmann and Bennewitz 2012; Kumar et al. 2015; Xiang et al. 2016). Limited empirical data exists for non-additive variance estimates, which varies greatly between organisms and can range from around 3-15% of total phenotypic variance in humans and animals (Misztal 1997; Zhu et al. 2015) to a third or more in plants (Kumar et al. 2015; Berguson et al. 2017; Calleja-Rodriguez et al. 2021). Adequate knowledge of non-additive genetic action is therefore of pivotal importance for a thorough understanding of the genetic architecture of complex traits, especially those that are fitness-related, and their evolutionary trajectory.

Motivated to better understand the prevalence and consequence of non-additive genetic action, we systematically compared the additivity and non-additivity in gene expression in *A. thaliana* F_1 hybrids. Consistent with findings in other systems (Fujimoto et al. 2012; Bell et al. 2013), we found non-additivity to be prevalent. Moreover, there was a prominent association between non-additivity and biomass on a cross-population scale, lending support to the theory of directional dominance being an underlying factor of emergent phenotypes in hybrids (Falconer and Mackay 1996).

Hybrid advantage was common in our F_1 collection, consistent with inferences from smaller sets of *A. thaliana* F_1 hybrids (Seymour et al. 2016; Oakley et al. 2019). In our system, hybrid

advantage seems to be driven in large part by non-additive gene expression. For many genes, when parent-hybrid trios are considered, the degree of non-additivity in F_1 expression is either positively or (more frequently) negatively associated with hybrid performance. GO enrichment points to repression of reproductive development and abiotic stress response, as well as increased photosynthesis as factors that support more robust growth in F_1 hybrids. The rewiring of transcriptional networks is likely to occur in *trans*, as binding motifs for a small number of transcription factors were enriched in the promoters of the focal genes.

In contrast, additive (i.e., near-MPV) expression itself does not correlate with the larger size of F_1 hybrids, hence probably does not directly contribute to hybrid advantage. The observation is consistent with the notion that additive variance is quickly driven to fixation in fitness traits (Merilä and Sheldon 1999). Additive expression appears to be an intrinsic property for certain genes, mainly enriched in cell-death and stress-response pathways, in F_1 hybrids, largely independent of specific parental combinations. Whether tighter control of biotic defense responses capacitates hybrid advantage requires further investigation.

It has long been postulated that heterosis is driven by directional dominance (Falconer and Mackay 1996). It is therefore noteworthy that we observed a consistent species-wide trend of non-additive expression leading to the relative gene-expression level in F_1 hybrids being more similar to the low-expression parents. With the proviso that we cannot rule out that the absolute transcript abundance of these genes were in fact increasing, our measurements do indicate a relative decrease in cellular transcript concentration, which could have consequences for molecular interactions (Gao et al. 2021; Koşar and Erbaş 2022). The abundance of up-stream rare alleles in these non-additively expressed genes further suggests that the change of expression had a genetic basis, as opposed to being merely a consequence of a common phenotype.

Another study recently reported high-parent expression of hub genes from regulatory networks of photosynthesis and cell cycles during early shoot development to be associated with a high degree of growth advantage in one specific F_1 hybrid (Liu et al. 2021). We similarly found above-MPV expression of photosynthetic function in the later phase of vegetative growth to be

358 positively correlated with increased growth. Both studies also agree in low-parent gene expression
359 being common in F_1 hybrids during the later stage of vegetative growth.

360 We observed putative deleterious effects (*i.e.*, strong deviation of gene expression from that
361 of the population mean) of rare alleles in upstream regulatory sequences, primarily in inbred
362 parental accessions, and to a lesser degree in F_1 hybrids, suggesting that rare-allele burden has
363 common effects in inbreds and hybrids alike. The correlation between rare-allele burden and gene
364 expression is more pronounced in additively than non-additively expressed genes. However, while
365 (the milder) rare-allele burden in non-additive genes is strongly associated with phenotypic
366 consequences in F_1 hybrids, this is not reflected in the behavior of the additive genes. We conclude
367 that concerted non-additive gene expression, rather than canalization via additive gene expression,
368 is a main driver of growth advantage in *A. thaliana* F_1 hybrids.

369 The use of RNA-seq enabled the parallel comparison of thousands of gene expression traits,
370 all quantified against the same scale. With this, we could define both "additive" and "non-additive"
371 genes by their expression at the population level, largely circumventing idiosyncratic behavior of
372 genes in a specific trio, enhancing our confidence that our observations can be generalized across
373 the species. By associating transcriptome changes and plant growth, we were also able to
374 characterize growth as a high-dimensional phenotype, with under-dominance as the predominant
375 type of gene action associated with growth advantage in F_1 hybrids. Our work provides another
376 step towards understanding molecular mechanisms and evolutionary forces that lead to dominance
377 complementation of rare regulatory alleles.

378 Materials and Methods

379 **Generation of genetic resource:** Accessions covering the entire species range were chosen from
380 the *A. thaliana* 1001 Genomes Project (1001 Genomes Consortium). F_1 hybrids used in this study
381 were generated via random crosses, either by randomly crossing individual accessions that reached
382 flowering stage at the same time (SHB1) (Vasseur et al. 2019), or according to a pre-generated

383 randomized crossing scheme after subjecting seedlings to a saturating (12 weeks) vernalization
384 under 4°C short-day conditions (SD, 8/16 hr photoperiod) to synchronize flowering (SHB2).
385 **Experimental design:** The first experiment (Fig. 1A, "SHB1") initially included 101 parent-F_1 trios of
386 altogether 286 distinct genotypes. Single plants were grown following an incomplete randomized
387 block design, with each tray as a block within which each genotype was sown as an adjacent pair.
388 The second experiment (Fig. 3A, "SHB2") included 40 parent-F_1 trios. Single plants were grown in
389 triplicates, following a split-block design where each block held 10 parent-F_1 trios with each row
390 consisting of one trio with duplicates of plants in adjacent pots. The trios within each block, and the
391 relative positions of genotypes within each trio were randomized. Plants were subjected to either a
392 mock or an artificial defense hormone treatment (see below). After accounting for germination,
393 survival, and initial filtering of RNA-seq outputs, 82 hybrids and 124 inbred parents in SHB1, and
394 32 trios in SHB2 remained for downstream analyses.
395 To minimize circadian bias, sowing for both experiments was scheduled in batches to ensure
396 that harvesting could be finished within a 30-minute window at the same hour for several
397 consecutive days. At 21 days after sowing, the healthiest appearing plant of each genotype was
398 used for RNA-seq, to ensure any sampling bias is systematically towards the same direction for both
399 inbreds and hybrids. Meanwhile rosette size measurements were obtained for the same individual
400 plants for which RNA-seq were performed.
401 For a list of genotypes analyzed in both experiments, see Data S1.
402 **Plant culture, treatment, and sampling**: Single plants were grown in a 1:1 mixture of calcined clay
403 media (Diamond Pro, Arlington, TX, USA) and vermiculite (Floragard, Oldenburg, Germany)
404 supplemented with liquid growth media (Conn et al. 2013). Plants were not vernalized, to ensure
405 that they remained in the vegetative growth phase. As a proxy of vegetative biomass (ref. (Vasseur
406 et al. 2018) and Fig. S1), the rosette area of 21-day old plants was measured. The full rosettes grown
407 under 16°C long-day (LD,16/8 photoperiod) were harvested and flash-frozen at 21 day-after-
408 germination (DAG).

409 Defense hormone treatment started 14 days after sowing. An analog of the defense hormone
410 salicylic acid (SA), BTH (acibenzolar-S-methyl, Sigma-Aldrich) was used, with optimal dose and
411 treatment scheme of the defense hormone that had been established in a pilot experiment on
412 multiple accessions (Fig. S2). Each 10×6-pot-tray block was the unit of treatment and plants were
413 treated by topical spraying every other day with either a mock solution (20 mL; ddH_2O, 0.1% DMSO,
414 0.006% Silwet) or a BTH solution (20 mL; 100 mM acibenzolar-S-methyl, 0.1% DMSO, 0.006%
415 Silwet), and covered for 1 hour with transparent plastic lids after spraying. A total of five treatments
416 were administered. Full rosettes were harvested and flash frozen at 21 DAG.

417 **Growth analysis**: Plant growth was monitored by daily image capture from the top of the trays using
418 the RAPA system (Capovilla et al. 2018). Rosette areas were acquired by automatic image
419 segmentation and counting of green pixels, supplemented with manual curation. The rosette size
420 estimates were then converted from pixel counts to mm^2 by multiplication with a calibration factor.

421 **RT-qPCR**: To establish defense hormone treatment and dosage, the effect of salicylic acid and BTH
422 application was tested by treating 18 accessions with Mock (ddH_2O, 0.1% DMSO, 0.006% Silwet),
423 350 mM SA and 100 mM BTH in 3 replicates, each with duplicated plants for phenotyping and
424 qPCR. After 5 treatments the rosettes were harvested in one set of plants to compare their sizes,
425 while the other set of plants were used for qPCR to compare the effect of 350 mM SA and 100 mM
426 BTH treatments. Specifically, RNA was extracted and reverse transcribed. qPCR was performed
427 using SYBER green (Thermo Scientific Maxima SYBR Green qPCR Master Mix (2x)) and primers for
428 *ACTIN2*, *UBC21*, *PR1* and *NPR1*. Normalization across plates was performed using the same set of
429 samples featured on all plates. The data were analyzed by calculating ΔΔCq (Fig. S14).

430 **RNA-seq**: RNA-seq libraries were constructed as described (Cambiagno et al. 2021), using 750 ng
431 total RNA from full rosettes as input. All libraries, each carrying a unique barcode combination were
432 pooled and sequenced in multiple single-end lanes on an Illumina HiSeq 3000 platform for a target
433 coverage of 5M reads per sample.

434 **RNA-seq read mapping and post-processing**: FASTQ files from multiple lanes were merged and
435 mapped to TAIR10 transcriptome using *RSEM* (*bowtie2*) with default parameters. Libraries with

436 more than 8M mapped reads were subsampled to 8M with *seqtk* prior to mapping. Transcripts
437 mapped to chloroplast, mitochondria, rDNA clusters, transposable elements (TEs) and
438 pseudogenes, as well as transcripts with effective length less than 150 nt were removed from the
439 raw *RSEM* count file. TPM (transcripts per million) counts were then re-estimated for the rest of the
440 genes. Libraries with fewer than 2M mapped reads and those identified as extreme outliers
441 following a principal-component analysis (PCA) of whole-transcriptome $\log_2$ (TPM) values were
442 excluded from further analysis. Gene lists were further filtered for average transcript abundance
443 (trimmed mean of $\log_2$ (TPM)>0.3) and coefficient of variance >0.15.

444 **Additive gene calling**: For SHB1 data, MPV of each gene was calculated for all complete Parent-F_1
445 trios by taking the arithmetic mean of the parental $\log_2$ (TPM). Linear regression was then performed
446 between corresponding F_1 expression value and the MPV. For SHB2, a linear-mixed model was
447 used to correct for treatment and batch effects. Genes were filtered for regression coefficient >0.5
448 and R^2 >0.4 for SHB1, and regression coefficient >0.4 and sigma <0.6 for SHB2. All thresholds were
449 determined by quantiles. Genes called in both SHB1 and SHB2 were taken as common additive
450 genes.

451 **Non-additive gene calling**: With SHB1, a population-wide MPV distribution was established for each
452 gene by calculating arithmetic means of $\log_2$ (TPM) between all possible pairwise combinations of
453 inbred accessions. Two-sided Kolmogorov-Smirnov test was performed per gene to test if the $\log_2$
454 (TPM) from the F_1 hybrids were drawn from the MPV distribution. Genes with q<0.001 (Benjamin-
455 Hochberg FDR) were considered as non-additively expressed genes.

456 **Bayesian modelling of non-additive expression and plant size**: non-additive genes from SHB1 were
457 clustered by K-means, with the optimal K determined by the elbow method. A linear-mixed-model
458 (LMM) spline was fitted using the *lme4* package(Bates et al. 2015) in R (ref. (R Core Team 2021)) for
459 gene expression:

460 GeneExpression~IsHybrid+Size+Size:IsHybrid+(IsHybrid|LibraryBatch),

461 in which *GeneExpression* is the z-scaled $\log_2$TPM, *IsHybrid* is a binary code of the hybrid/inbred
462 identity, *Size* is the z-score of rosette size at sampling. Natural cubic splines were modeled for *Size*

463 and *Size-IsHybrid* interaction. The 95% credible intervals for the parameter estimates were
464 established with 10,000 iterations of Bayesian simulation using the *arm* package(Andrew Gelman,
465 Yu-Sung Su, Masanao Yajima, Jennifer Hill, Maria Grazia Pittau, Jouni Kerman, Tian Zheng, Vincent
466 Dorie 2021).

467 **BTH responsive genes:** The effect of BTH treatment on gene expression was identified by LMM:

468 GeneExpression~Treatment+IsHybrid+Treatment*IsHybrid+(1|PlantBatch).

469 To establish a significant threshold, 10,000 permutations were performed for each gene, and the
470 empirical p-value was corrected with Benjamin-Hochberg FDR. Genes with q<0.001 were kept as
471 BTH responsive genes (n=8,797) and examined for their size-MPH correlation.

472 **Expression-plant size MPH correlation**: Expression-MPH and size-MPH were calculated per trio by
473 calculating the per-gene expression and rosette area difference between F_1 and the MPV in
474 corresponding treatments and replicates. Size MPH-to-expression MPH regression spline was
475 acquired separately for both treatments. An initial round of K-means clustering was performed on
476 the resulting spline coefficients, with the optimal K determined as the division with the highest Dunn
477 index which allows no more than 25% of the clusters carrying less than 5% of the genes. Resulting
478 clusters were inspected and removed if size and expression MPH do not co-vary. The remaining
479 genes (n=6,371) were re-clustered with the same criteria, and the resulting clusters were manually
480 sorted based on size-expression covariation into 12 general categories (Data S3, Fig. 4D, Fig. S9).

481 **Size-MPH covariation test**: To establish the significance of the size-expression correlation, we
482 performed a Wilcoxon signed-rank test on the genes in each of the 61 clusters (Fig. 4B). For each
483 "none" cluster, each gene within the cluster was used as a data point, and the mean rosette size of
484 4 plants having the lowest and the highest expression MPH of the gene was calculated. The average
485 rosette size corresponding to the two extremes of expression MPH were then compared with a two-
486 sided Wilcoxon signed-rank test. Likewise, for "positive" and "negative" clusters, one-sided tests
487 were used to test for significant differences between average rosette size corresponding to the two
488 extremes of expression MPH within individual clusters. For "quadratic" clusters, separate one-sided
489 tests were performed comparing the samples with extreme expression MPH against those with

490 median expression MPH. Bonferroni correction was used to control for multiple hypothesis testing.
491 The test revealed that our sorting procedure erred on the conservative side: while the top and
492 bottom deciles were significantly different for 17 clusters assigned to the "none" category, only 6
493 of the "none" clusters were misassigned as "positive", and none were misassigned as "negative"
494 (Bonferroni corrected **α**<0.001, Data S3). The evidence for truly quadratic correlations was less clear.
495 **GO enrichment:** GO enrichment was performed using the *Agrigo* v2 platform(Tian et al. 2017), with
496 all gene IDs that passed our initial filtering (n=14,067, TAIR10 annotation) as background against
497 plant GOslim database. Fisher's Exact Test was used, and the enrichment p-value was corrected
498 using Yekutieli FDR. The enrichment results were visualized with the built-in DAG-drawer of *Agrigo*
499 v2.
500 **Rare allele analysis**: Rare (MAF<0.05), biallelic SNPs 1 kb upstream of gene features were subset
501 from the SNP annotations of the 1001 Genomes Project (1001 Genomes Consortium. Electronic
502 address: magnus.nordborg@gmi.oeaw.ac.at and 1001 Genomes Consortium 2016). Genotype
503 information at these SNPs were acquired for the accessions used in SHB2, and the sum of these
504 rare SNPs upstream of each gene were calculated per accession. For F_1 hybrids, upstream rare-
505 allele count was determined by the mean of the rare-allele counts of both parents.
506 Samples, separated by inbred parents/F_1 hybrids and with/without BTH treatment, were
507 ranked for their expression values for each gene within a gene list of interest. For each given rank,
508 a gene-list mean upstream rare-allele count was acquired by averaging across all samples received
509 the same rank in any of the genes within the gene list. Relationships between gene-list mean
510 upstream rare-allele count and expression rank were examined by LOWESS regression and tested
511 with Wilcoxon signed rank sum test between the top and bottom decile of the expression rank.
512 Likewise, an average rosette-size MPH for each rank was calculated for the gene list, and
513 the Pearson correlation was acquired between average rosette-size MPH and upstream rare-allele
514 count.
515 **Motif enrichment and *de novo* motif finding**: Motif enrichment and *de novo* motif finding was
516 carried out using *HOMER* v4.10.4 (ref. (Heinz et al. 2010)) with TAIR10 reference genome and gene

517 annotation. For every set of candidate genes, genomic sequences 1 kb upstream from the
518 transcription start site (TSS) and 1 kb downstream from the transcription termination site (TTS) were
519 indexed from the strand-specific gene coordinates. Both assays were performed by using the
520 *findMotifsGenome.pl* function and *HOMER*'s in-built plant promoter motif database as reference:

521 *findMotifsGenome.pl* [geneset_promoter_coord.bed] [TAIR10_customref] [motif_outputdir]
522 *-size given* -S 15 *-preparse -mcheck* [homer_database/data/knownTFs/plant/all.motifs]

523 The top known motif hit (in all cases $p \leq 10^{-10}$) from each candidate set was then used for a second
524 motif enrichment step, where the promoters and downstream sequences were searched for the
525 significant motif using *HOMER*'s *annotatePeaks.pl* function:

526 *annotatePeaks.pl* [geneset_promoter_downstream.bed] [TAIR10_customref]
527 *-m* [motif_outputdir]/knownResults/known1.motif *-size given -nmotifs -mbed*
528 [output1.bed] > [output1.txt],

529 to generate corresponding genomic coordinates, and subsequently associated back to the genes
530 containing the motif of interest in their regulatory regions (*bedtools* v2.26.0 intersect)(Quinlan and
531 Hall 2010).

532 Acknowledgements

533 We thank members of the Weigel lab for assistance with sample collection, and James Birchler,
534 Chang Liu, François Vasseur, Ulrich Lutz, Rebecca Schwab, and Yiliang Ding for helpful discussions.
535 This work was supported by the Max Planck Society.

536 Author Contributions

537 Conceptualization – WY, DW; Methodology – WY, IB; Experiment – WY, FB, SS, RK; Data analysis
538 – WY, FB, TS; Writing – original draft: WY, FB; Writing – review & editing – WY, DW.

539 Competing Interests

540 D.W. holds equity in Computomics, which advises breeders.

541 Data and Material Availability

542 Raw sequencing data is available at the ENA under the accession ERA9420648 and ERA9420737.

543 Code to generate the results is available at: https://github.com/weigelworld/SigHeterosis.

544 Supplementary Data Sets

545 **DataS1**.xlsx Sequenced and analyzed genotypes from SHB1 and SHB2

546 **DataS2**.txt Non-additive genes called in SHB1, and their cluster identity

547 **DataS3**.xlsx Wilcoxon rank sum test on the size-expression MPH spline clusters

548 **DataS4**.txt Genes negatively associated with heterosis under BTH or mock + BTH conditions

549 ("negative genes")

550 **DataS5**.txt Genes positively associated with heterosis under both mock and BTH conditions

551 ("positive genes")

552 **DataS6**.txt 300 common additive genes

553 References

554 1001 Genomes Consortium. 2016. 1,135 Genomes Reveal the Global Pattern of Polymorphism in
555 Arabidopsis thaliana. *Cell* 166:481–491.
556 Albert FW, Kruglyak L. 2015. The role of regulatory variation in complex traits and disease. *Nat.*
557 *Rev. Genet.* 16:197–212.
558 Andrew Gelman, Yu-Sung Su, Masanao Yajima, Jennifer Hill, Maria Grazia Pittau, Jouni Kerman,
559 Tian Zheng, Vincent Dorie. 2021. Data Analysis Using Regression and Multilevel/Hierarchical
560 Models [R package arm version 1.12-2]. Available from: https://cran.r-
561 project.org/web/packages/arm/index.html
562 Bates D, Mächler M, Bolker B, Walker S. 2015. Fitting Linear Mixed-Effects Models Using lme4.
563 *Journal of Statistical Software, Articles* 67:1–48.
564 Batts GR, Morison JIL, Ellis RH, Hadley P, Wheeler TR. 1997. Effects of CO2 and temperature on
565 growth and yield of crops of winter wheat over four seasons. In: van Ittersum MK, van de Geijn
566 SC, editors. Developments in Crop Science. Vol. 25. Elsevier. p. 67–76.
567 Bell GDM, Kane NC, Rieseberg LH, Adams KL. 2013. RNA-seq analysis of allele-specific expression,
568 hybrid effects, and regulatory divergence in hybrids compared with their parents from natural
569 populations. *Genome Biol. Evol.* 5:1309–1323.

570 Berguson WE, McMahon BG, Riemenschneider DE. 2017. Additive and Non-Additive Genetic
571 Variances for Tree Growth in Several Hybrid Poplar Populations and Implications Regarding
572 Breeding Strategy. *Silvae Genet.* 66:33–39.
573 Birchler JA, Auger DL, Riddle NC. 2003. In search of the molecular basis of heterosis. *Plant Cell*
574 15:2236–2239.
575 Bomblies K, Lempe J, Epple P, Warthmann N, Lanz C, Dangl JL, Weigel D. 2007. Autoimmune
576 Response as a Mechanism for a Dobzhansky-Muller-Type Incompatibility Syndrome in Plants.
577 *PLoS Biol.* 5:e236.
578 Bomblies K, Weigel D. 2007. Hybrid necrosis: autoimmunity as a potential gene-flow barrier in plant
579 species. *Nat. Rev. Genet.* 8:382–393.
580 Braendle C, Heyland A, Flatt T. 2011. Integrating mechanistic and evolutionary analysis of life
581 history variation. *Mechanisms of life history evolution. The genetics and physiology of life history*
582 *traits and trade-offs*:3–10.
583 Calleja-Rodriguez A, Chen Z, Suontama M, Pan J, Wu HX. 2021. Genomic Predictions With
584 Nonadditive Effects Improved Estimates of Additive Effects and Predictions of Total Genetic
585 Values in Pinus sylvestris. *Front. Plant Sci.* 12:666820.
586 Cambiagno DA, Giudicatti AJ, Arce AL, Gagliardi D, Li L, Yuan W, Lundberg DS, Weigel D,
587 Manavella PA. 2021. HASTY modulates miRNA biogenesis by linking pri-miRNA transcription
588 and processing. *Mol. Plant* 14:426–439.
589 Capovilla G, Delhomme N, Collani S, Shutava I, Bezrukov I, Symeonidi E, de Francisco Amorim M,
590 Laubinger S, Schmid M. 2018. PORCUPINE regulates development in response to temperature
591 through alternative splicing. *Nat Plants* 4:534–539.
592 Chae E, Bomblies K, Kim S-T, Karelina D, Zaidem M, Ossowski S, Martín-Pizarro C, Laitinen RAE,
593 Rowan BA, Tenenboim H, et al. 2014. Species-wide genetic incompatibility analysis identifies
594 immune genes as hot spots of deleterious epistasis. *Cell* 159:1341–1351.
595 Conn SJ, Hocking B, Dayod M, Xu B, Athman A, Henderson S, Aukett L, Conn V, Shearer MK,
596 Fuentes S, et al. 2013. Protocol: optimising hydroponic growth systems for nutritional and
597 physiological analysis of Arabidopsis thaliana and other plants. *Plant Methods* 9:4.
598 Crow JF. 2010. On epistasis: why it is unimportant in polygenic directional selection. *Philos. Trans.*
599 *R. Soc. Lond. B Biol. Sci.* 365:1241–1244.
600 Elings A, White JW, Edmeades GO. 1997. Options for breeding for greater maize yields in the
601 tropics. In: van Ittersum MK, van de Geijn SC, editors. Developments in Crop Science. Vol. 25.
602 Elsevier. p. 155–168.
603 Falconer DS, Mackay TFC. 1996. Introduction to quantitative genetics, Longman. *Essex, England.*
604 Fujimoto R, Taylor JM, Shirasawa S, Peacock WJ, Dennis ES. 2012. Heterosis of Arabidopsis hybrids
605 between C24 and Col is associated with increased photosynthesis capacity. *Proc. Natl. Acad.*
606 *Sci. U. S. A.* 109:7109–7114.
607 Gao R, Helfant LJ, Wu T, Li Z, Brokaw SE, Stock AM. 2021. A balancing act in transcription regulation
608 by response regulators: titration of transcription factor activity by decoy DNA binding sites.
609 *Nucleic Acids Res.* 49:11537–11549.

610 Gonzalez DH. 2015. Plant Transcription Factors: Evolutionary, Structural and Functional Aspects.
611 Academic Press
612 González R, Butković A, Rivarez MPS, Elena SF. 2020. Natural variation in Arabidopsis thaliana
613 rosette area unveils new genes involved in plant development. *Sci. Rep.* 10:17600.
614 Heinz S, Benner C, Spann N, Bertolino E, Lin YC, Laslo P, Cheng JX, Murre C, Singh H, Glass CK.
615 2010. Simple combinations of lineage-determining transcription factors prime cis-regulatory
616 elements required for macrophage and B cell identities. *Mol. Cell* 38:576–589.
617 Hemani G, Knott S, Haley C. 2013. An evolutionary perspective on epistasis and the missing
618 heritability. *PLoS Genet.* 9:e1003295.
619 Jeffrey Chen Z. 2013. Genomic and epigenetic insights into the molecular bases of heterosis. *Nat.*
620 *Rev. Genet.* 14:471–482.
621 Julkowska MM, Klei K, Fokkens L, Haring MA, Schranz ME, Testerink C. 2016. Natural variation in
622 rosette size under salt stress conditions corresponds to developmental differences between
623 Arabidopsis accessions and allelic variation in the LRR-KISS gene. *J. Exp. Bot.* 67:2127–2138.
624 Korves TM, Schmid KJ, Caicedo AL, Mays C, Stinchcombe JR, Purugganan MD, Schmitt J. 2007.
625 Fitness effects associated with the major flowering time gene FRIGIDA in Arabidopsis thaliana in
626 the field. *Am. Nat.* 169:E141–E157.
627 Koşar Z, Erbaş A. 2022. Can the Concentration of a Transcription Factor Affect Gene Expression?
628 *Frontiers in Soft Matter* [Internet] 2. Available from:
629 https://www.frontiersin.org/articles/10.3389/frsfm.2022.914494
630 Kremling KAG, Chen S-Y, Su M-H, Lepak NK, Romay MC, Swarts KL, Lu F, Lorant A, Bradbury PJ,
631 Buckler ES. 2018. Dysregulation of expression correlates with rare-allele burden and fitness loss
632 in maize. *Nature* 555:520–523.
633 Kumar S, Molloy C, Muñoz P, Daetwyler H, Chagné D, Volz R. 2015. Genome-Enabled Estimates of
634 Additive and Nonadditive Genetic Variances and Prediction of Apple Phenotypes Across
635 Environments. *G3* 5:2711–2718.
636 Landry CR, Hartl DL, Ranz JM. 2007. Genome clashes in hybrids: insights from gene expression.
637 *Heredity* 99:483–493.
638 Li S. 2015. The Arabidopsis thaliana TCP transcription factors: A broadening horizon beyond
639 development. *Plant Signal. Behav.* 10:e1044192.
640 Liu W, He G, Deng XW. 2021. Biological pathway expression complementation contributes to
641 biomass heterosis in Arabidopsis. *Proc. Natl. Acad. Sci. U. S. A.* [Internet] 118. Available from:
642 http://dx.doi.org/10.1073/pnas.2023278118
643 Mackay TFC, Stone EA, Ayroles JF. 2009. The genetics of quantitative traits: challenges and
644 prospects. *Nat. Rev. Genet.* 10:565–577.
645 Merilä J, Sheldon BC. 1999. Genetic architecture of fitness and nonfitness traits: empirical patterns
646 and development of ideas. *Heredity* 83 (Pt 2):103–109.
647 Miller M, Song Q, Shi X, Juenger TE, Chen ZJ. 2015. Natural variation in timing of stress-responsive
648 gene expression predicts heterosis in intraspecific hybrids of Arabidopsis. *Nat. Commun.* 6:7453.

649 Misztal I. 1997. Estimation of Variance Components with Large-Scale Dominance Models. *J. Dairy*
650 *Sci.* 80:965–974.
651 Oakley CG, Lundemo S, Ågren J, Schemske DW. 2019. Heterosis is common and inbreeding
652 depression absent in natural populations of Arabidopsis thaliana. *J. Evol. Biol.* [Internet].
653 Available from: http://dx.doi.org/10.1111/jeb.13441
654 Quinlan AR, Hall IM. 2010. BEDTools: a flexible suite of utilities for comparing genomic features.
655 *Bioinformatics* 26:841–842.
656 R Core Team. 2021. R: A language and environment for statistical computing. R Foundation for
657 Statistical Computing, Vienna, Austria. Available from: https://www.R-project.org/
658 Rieseberg LH, Kim S-C, Randell RA, Whitney KD, Gross BL, Lexer C, Clay K. 2007. Hybridization
659 and the colonization of novel habitats by annual sunflowers. *Genetica* 129:149–165.
660 Seymour DK, Chae E, Grimm DG, Martín Pizarro C, Habring-Müller A, Vasseur F, Rakitsch B,
661 Borgwardt KM, Koenig D, Weigel D. 2016. Genetic architecture of nonadditive inheritance in
662 Arabidopsis thaliana hybrids. *Proc. Natl. Acad. Sci. U. S. A.* 113:E7317–E7326.
663 Su G, Christensen OF, Ostersen T, Henryon M, Lund MS. 2012. Estimating additive and non-
664 additive genetic variances and predicting genetic merits using genome-wide dense single
665 nucleotide polymorphism markers. *PLoS One* 7:e45293.
666 Tian T, Liu Y, Yan H, You Q, Yi X, Du Z, Xu W, Su Z. 2017. agriGO v2.0: a GO analysis toolkit for the
667 agricultural community, 2017 update. *Nucleic Acids Res.* 45:W122–W129.
668 Varona L, Legarra A, Toro MA, Vitezica ZG. 2018. Non-additive Effects in Genomic Selection. *Front.*
669 *Genet.* 9:78.
670 Vasseur F, Bresson J, Wang G, Schwab R, Weigel D. 2018. Image-based methods for phenotyping
671 growth dynamics and fitness components in Arabidopsis thaliana. *Plant Methods* 14:63.
672 Vasseur F, Fouqueau L, de Vienne D, Nidelet T, Violle C, Weigel D. 2019. Nonlinear phenotypic
673 variation uncovers the emergence of heterosis in Arabidopsis thaliana. *PLoS Biol.* 17:e3000214.
674 Vogel A, Ebeling A, Gleixner G, Roscher C, Scheu S, Ciobanu M, Koller-France E, Lange M, Lochner
675 A, Meyer ST, et al. 2019. Chapter Seven - A new experimental approach to test why biodiversity
676 effects strengthen as ecosystems age. In: Eisenhauer N, Bohan DA, Dumbrell AJ, editors.
677 Advances in Ecological Research. Vol. 61. Academic Press. p. 221–264.
678 Wainberg M, Sinnott-Armstrong N, Mancuso N, Barbeira AN, Knowles DA, Golan D, Ermel R,
679 Ruusalepp A, Quertermous T, Hao K, et al. 2019. Opportunities and challenges for
680 transcriptome-wide association studies. *Nat. Genet.* 51:592–599.
681 Wellmann R, Bennewitz J. 2012. Bayesian models with dominance effects for genomic evaluation
682 of quantitative traits. *Genet. Res.* 94:21–37.
683 Wieters B, Steige KA, He F, Koch EM, Ramos-Onsins SE, Gu H, Guo Y-L, Sunyaev S, de Meaux J.
684 2021. Polygenic adaptation of rosette growth in Arabidopsis thaliana. *PLoS Genet.* 17:e1008748.
685 Xiang T, Christensen OF, Vitezica ZG, Legarra A. 2016. Genomic evaluation by including dominance
686 effects and inbreeding depression for purebred and crossbred performance with an application
687 in pigs. *Genet. Sel. Evol.* 48:92.

Yang M, Wang X, Ren D, Huang H, Xu M, He G, Deng XW. 2017. Genomic architecture of biomass heterosis in Arabidopsis. *Proc. Natl. Acad. Sci. U. S. A.* [Internet]. Available from: http://dx.doi.org/10.1073/pnas.1705423114

Zhu Z, Bakshi A, Vinkhuyzen AAE, Hemani G, Lee SH, Nolte IM, van Vliet-Ostaptchouk JV, Snieder H, LifeLines Cohort Study, Esko T, et al. 2015. Dominance genetic variation contributes little to the missing heritability for human complex traits. *Am. J. Hum. Genet.* 96:377–385.

Zuk O, Hechter E, Sunyaev SR, Lander ES. 2012. The mystery of missing heritability: Genetic interactions create phantom heritability. *Proc. Natl. Acad. Sci. U. S. A.* 109:1193–1198.

Supplementary Figures

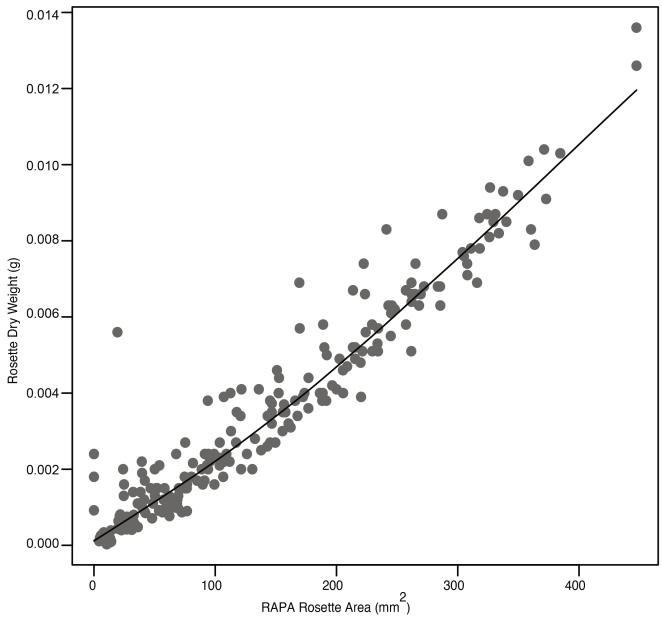

Figure S1. Rosette area serves as a good predictor of rosette biomass. Pearson correlation coefficient (R= 0.96, p<2.2e-16) of biomass (g) with rosette area (mm^2) as measured on the RAPA system at 21 days after sowing of 221 individuals of mixed genotypes (grey dots), and LOWESS trendline.

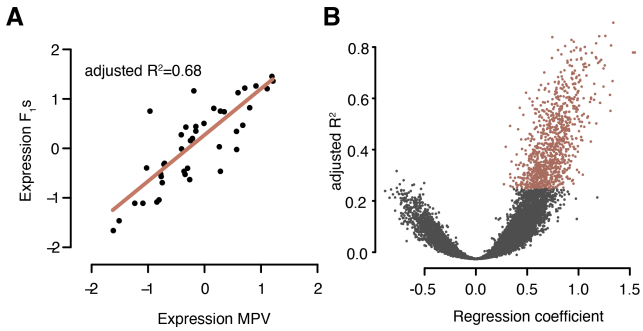

Figure S2. Linear-model-based additive gene calling. A. One representative additive gene (At5G43740, a CC-NBS-LRR class disease resistance protein, Non-additive rank: 16,574) whose expression in F_1 hybrids closely correlates with calculated mid-parent value, both showed as z-score. The red line shows the regression line. B. Volcano plot of R^2 value of each gene plotted against the corresponding linear-regression coefficient. Red dots show genes that passed the filtering threshold.

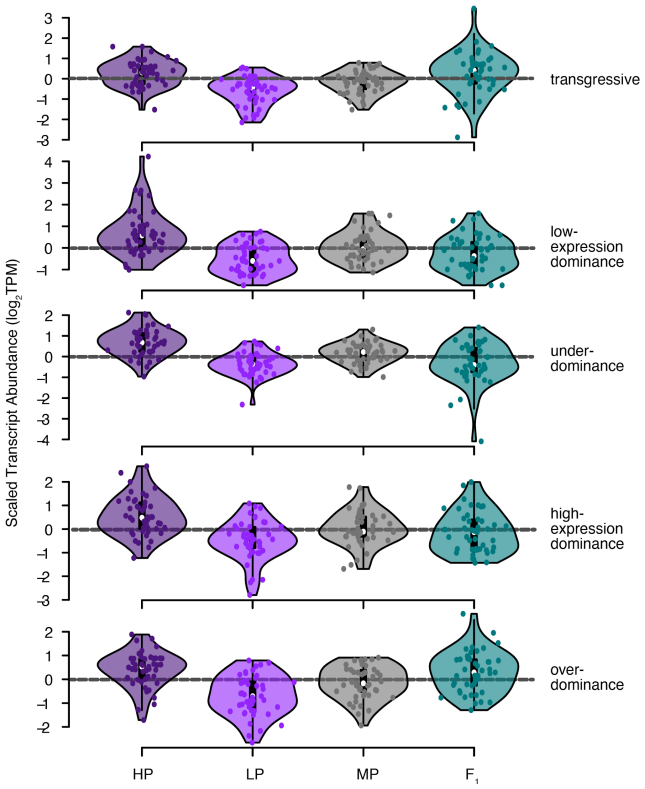

Figure S3. Examples showing that non-additive genes exhibit various forms of dominance in F_1s. From top: AT5G07960, AT3G61170, AT2G17670, AT2G27510, AT4G12970.

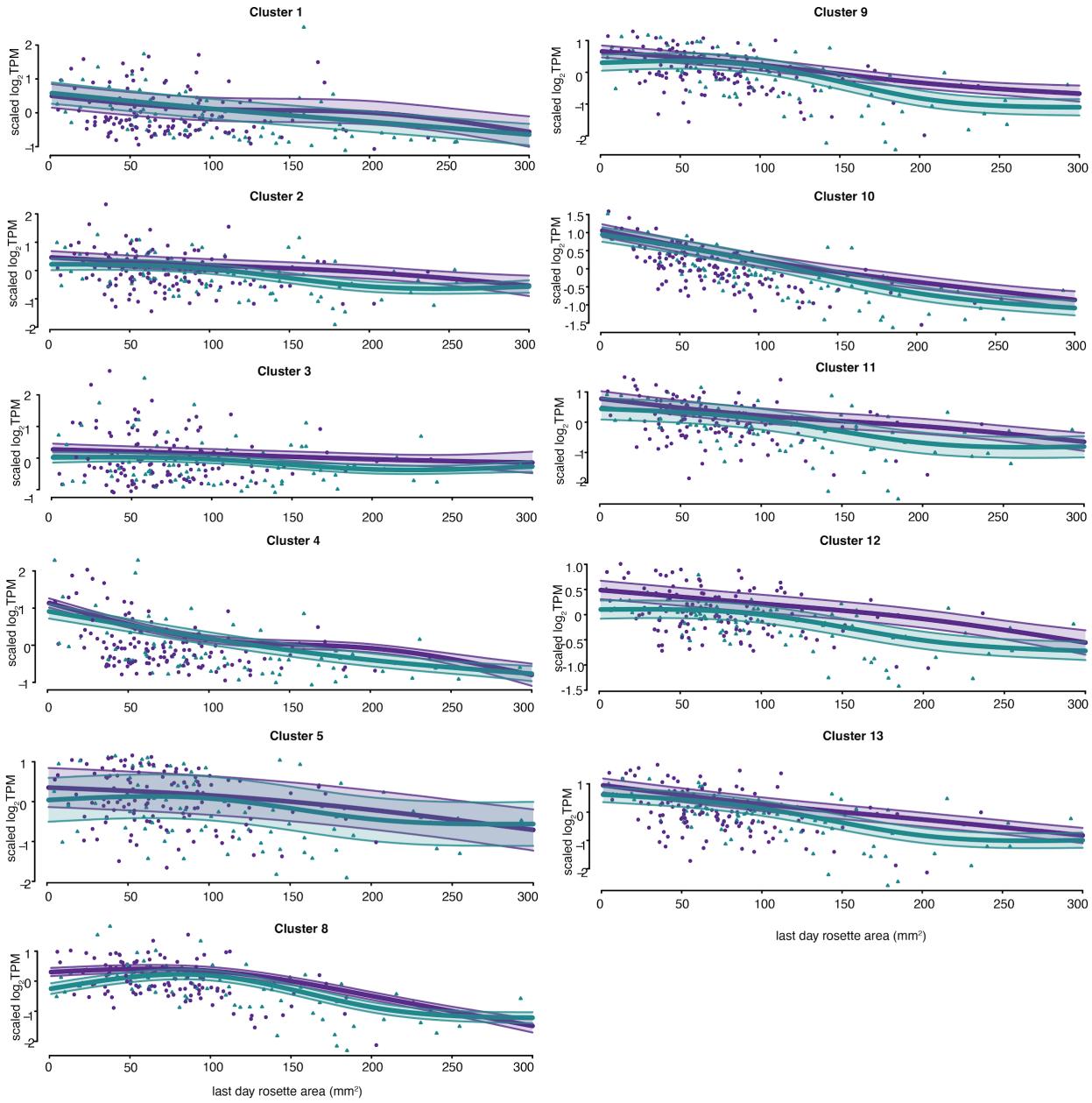

712

713 **Figure S4. BTH treatment reduced rosette size in both inbreds and F_1s.** LMM spline fitting of cluster mean
714 expression levels with 95% Bayesian credible intervals for non-additive gene clusters not shown in Fig. 3.
715 Mean expression level across all genes within a cluster for inbred parents (purple dots) and F_1 hybrids
716 (turquoise dots) against last day rosette area (mm^2) were plotted. Clusters 1-5 showed little rosette size-
717 expression level association, while clusters 8-13 showed monotonic decrease of cluster mean expression level
718 with increased plant size. While F_1 hybrids exhibited the same trend as the inbred parents, the mean
719 expression levels are consistently lower in F_1 hybrids across the entire rosette size range for cluster 8-13.

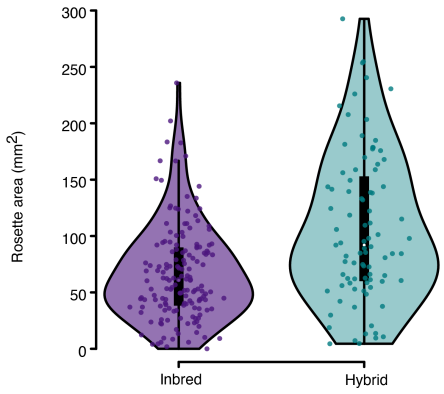

720

721 **Figure S5. Rosette size in inbred parental lines and F_1 hybrids.** The F_1 population has significantly more large
722 individuals than the inbred population ($p=2x10^{-5}$, Two-tailed Kolmogorov-Smirnov). F_1s: 107.1±66.1 mm^2,
723 n=82; parents: 67.2±42.5 mm^2, n=124. In a comparison of randomly chosen F_1s and inbreds, the F_1 hybrid
724 was twice as likely than the inbred to be the larger individual (Cliff's delta=0.33).

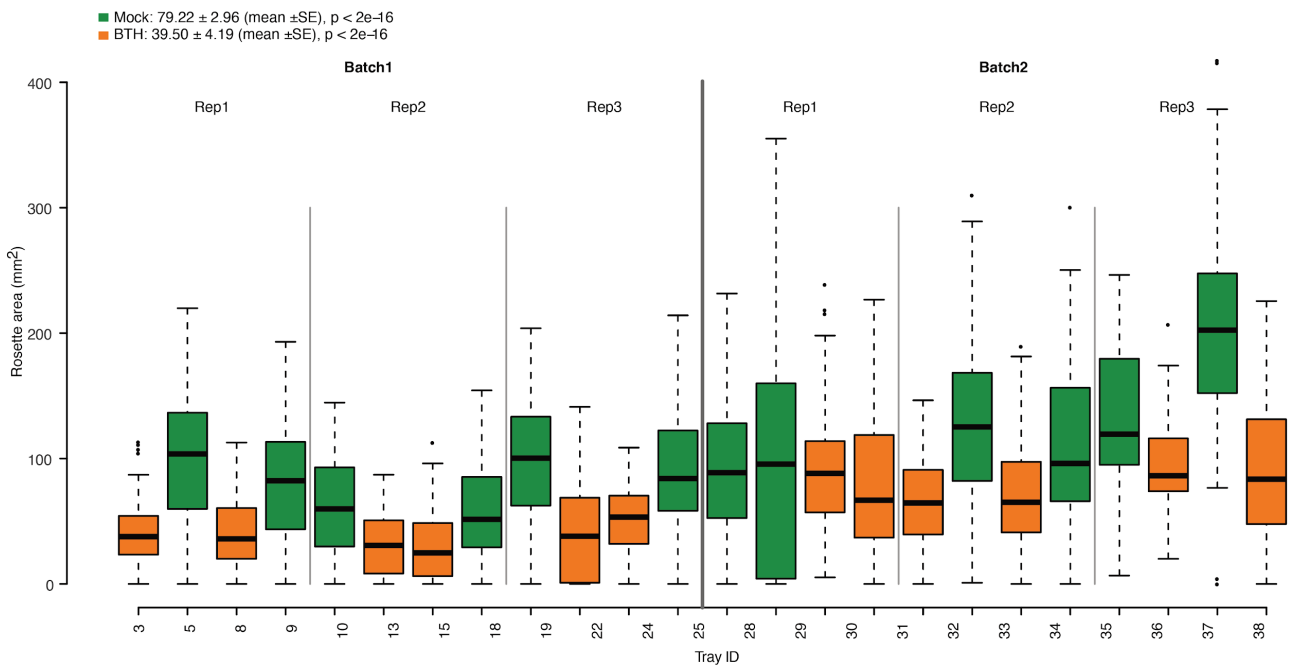

Figure S6. Consistent and significant reduction in rosette area by BTH in both batches of the SHB2 experiment. Each tray was a treatment unit. Shown are boxplots of rosette area (mm^2) in each tray with mock (green) or BTH treatment (orange). Only trays with parent-hybrid trios further used for transcriptome analysis are included. The rosette area after treatment with BTH was reduced compared to mock treatment (2-way nested ANOVA, mock: 79.2 ± 3.0 mm^2, BTH treatment: 39.5 ± 4.2 mm^2; $p < 10^{-16}$).

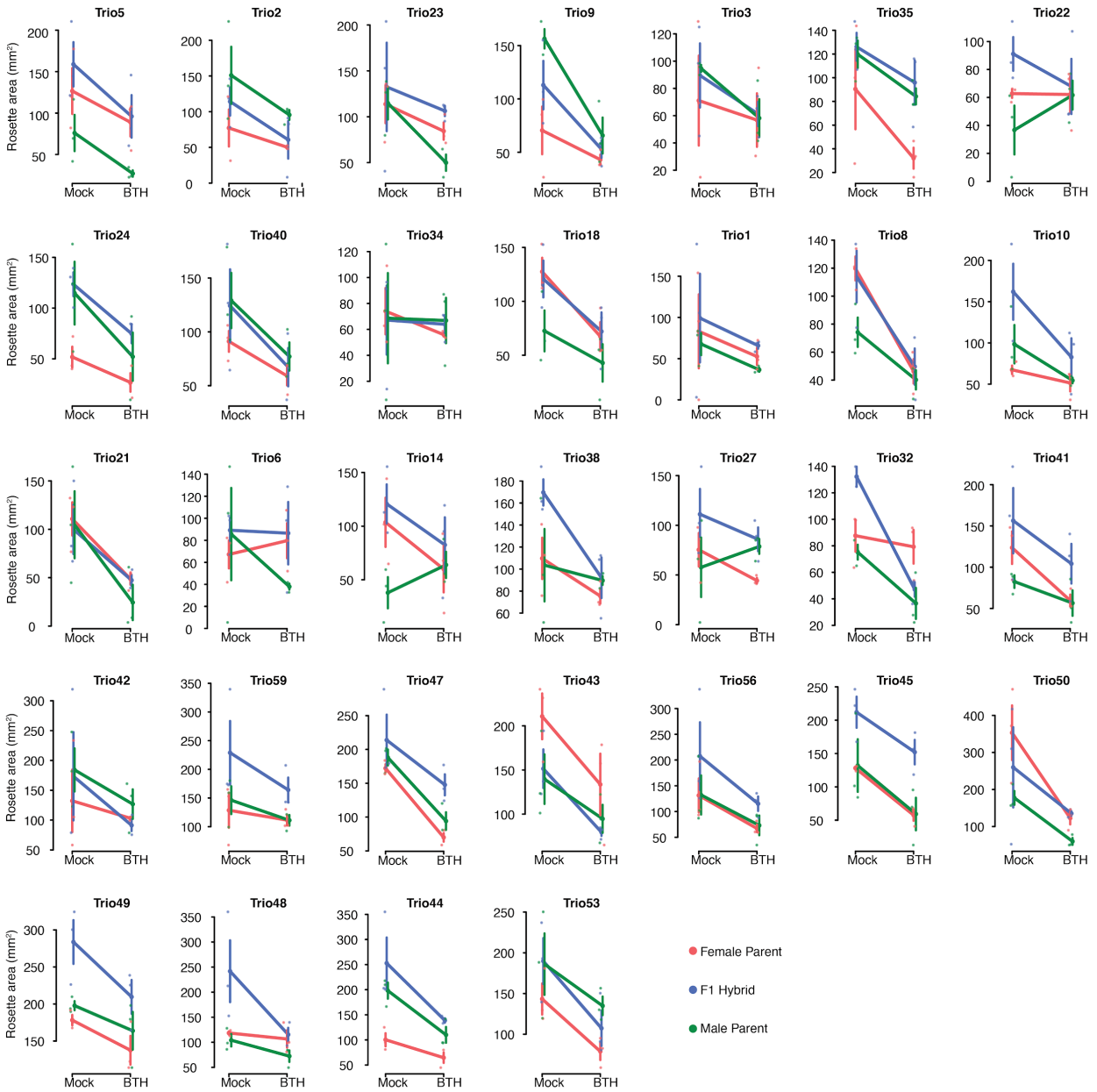

Figure S7. Reaction norm of rosette area (mm²) after mock and BTH treatments for all inbred parents and F_1 hybrid trios. Solid lines connected the mean rosette area under the two treatments, with the dots illustrating individual rosette area of each plant and the error bars showing standard deviation of the biological replicates.

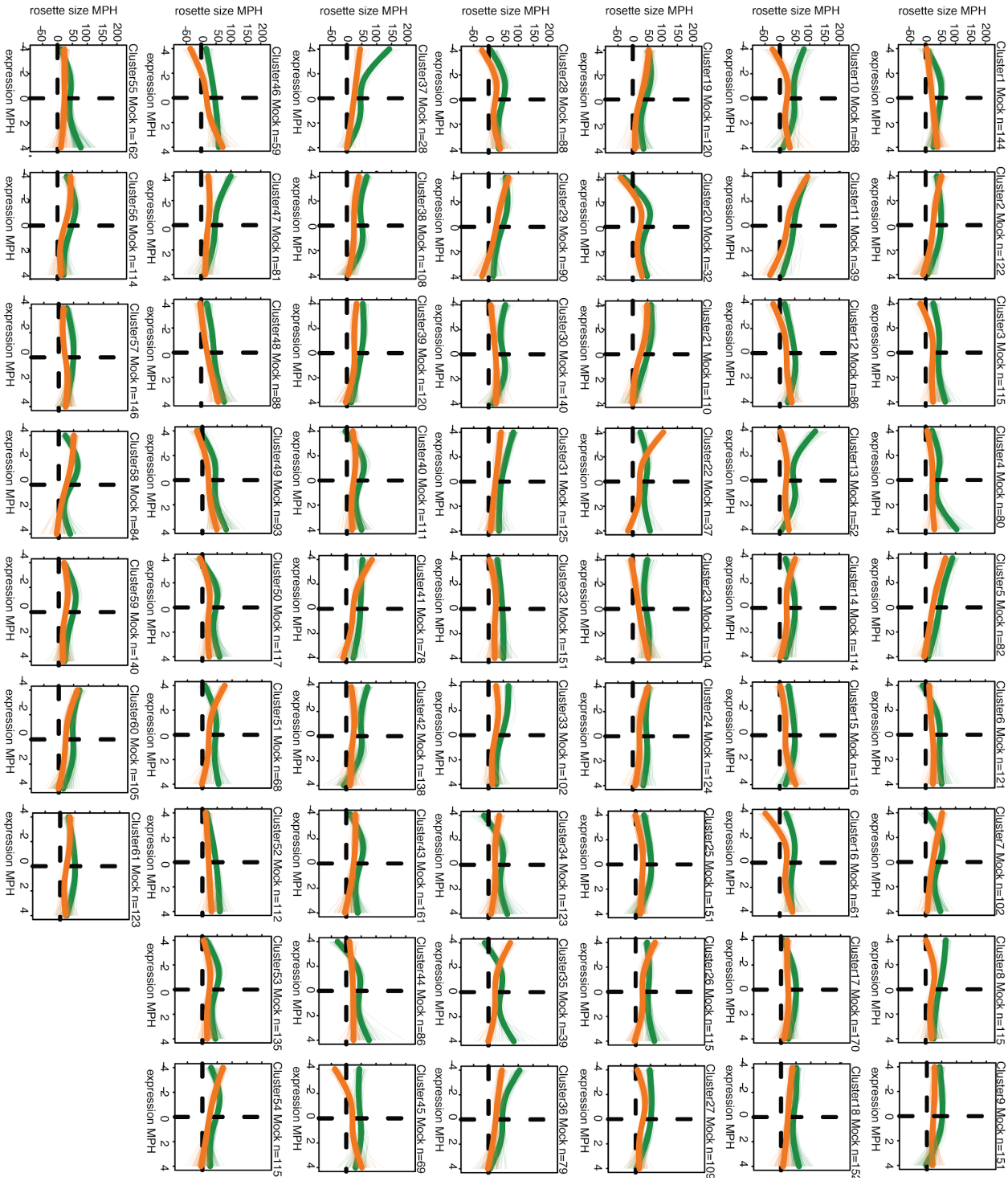

Figure. S8. BTH-responsive genes sorted into 61 clusters. Genes were sorted based on spline regression of rosette area MPH (mm^2) to their expression MPH across all trios. Shown are a graphic representation of the clusters. Each thin line represents a gene, and the thick line represents cluster mean (green: mock, orange: BTH). The 61 clusters were subsequently sorted into 12 general categories based on the regression trends in mock and BTH treatments.

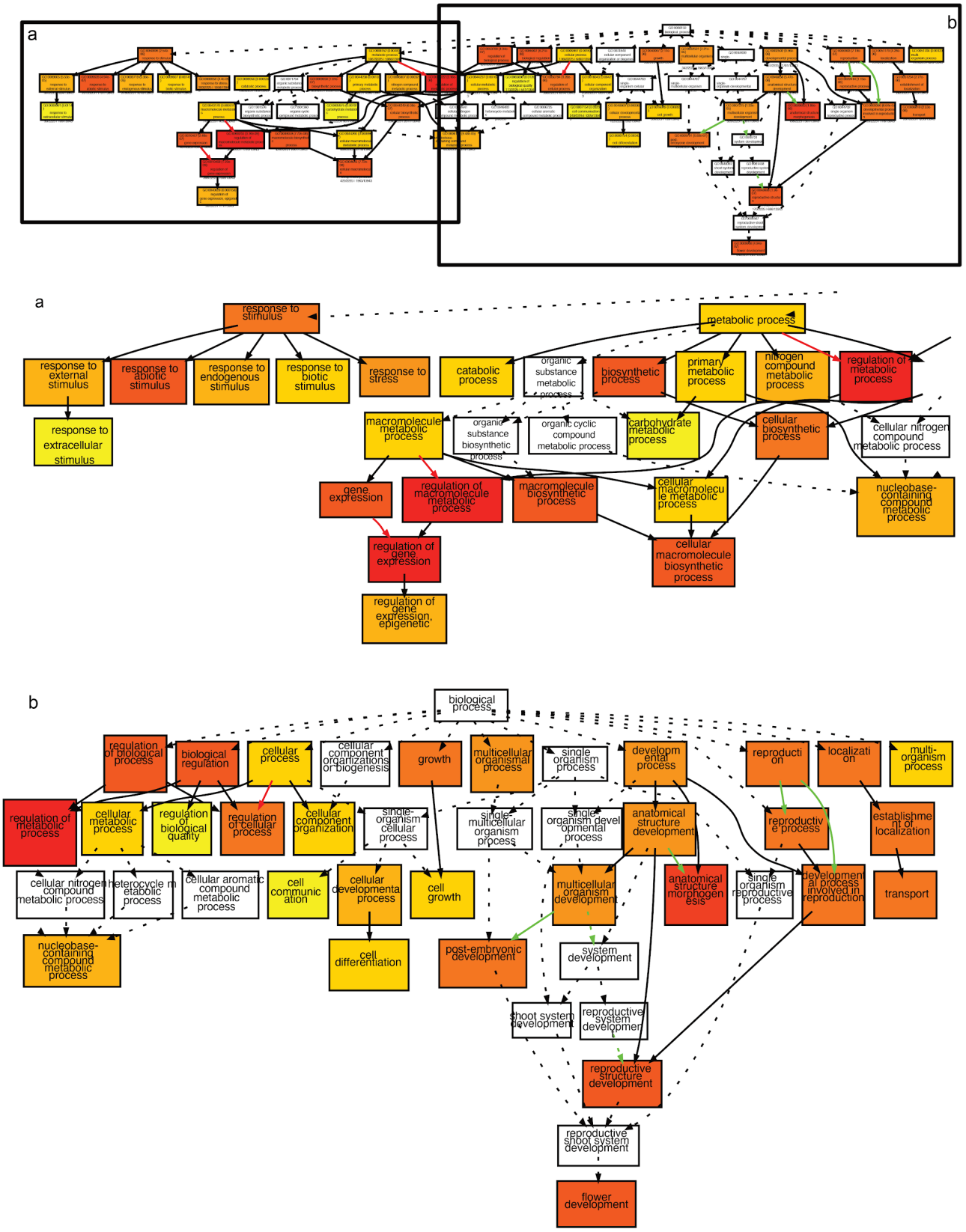

741

742 **Figure S9. GO enrichment for the negative genes.** Enlarged rendering of Fig. 4D. The diagram was split into

743 two parts (a and b) for improved legibility.

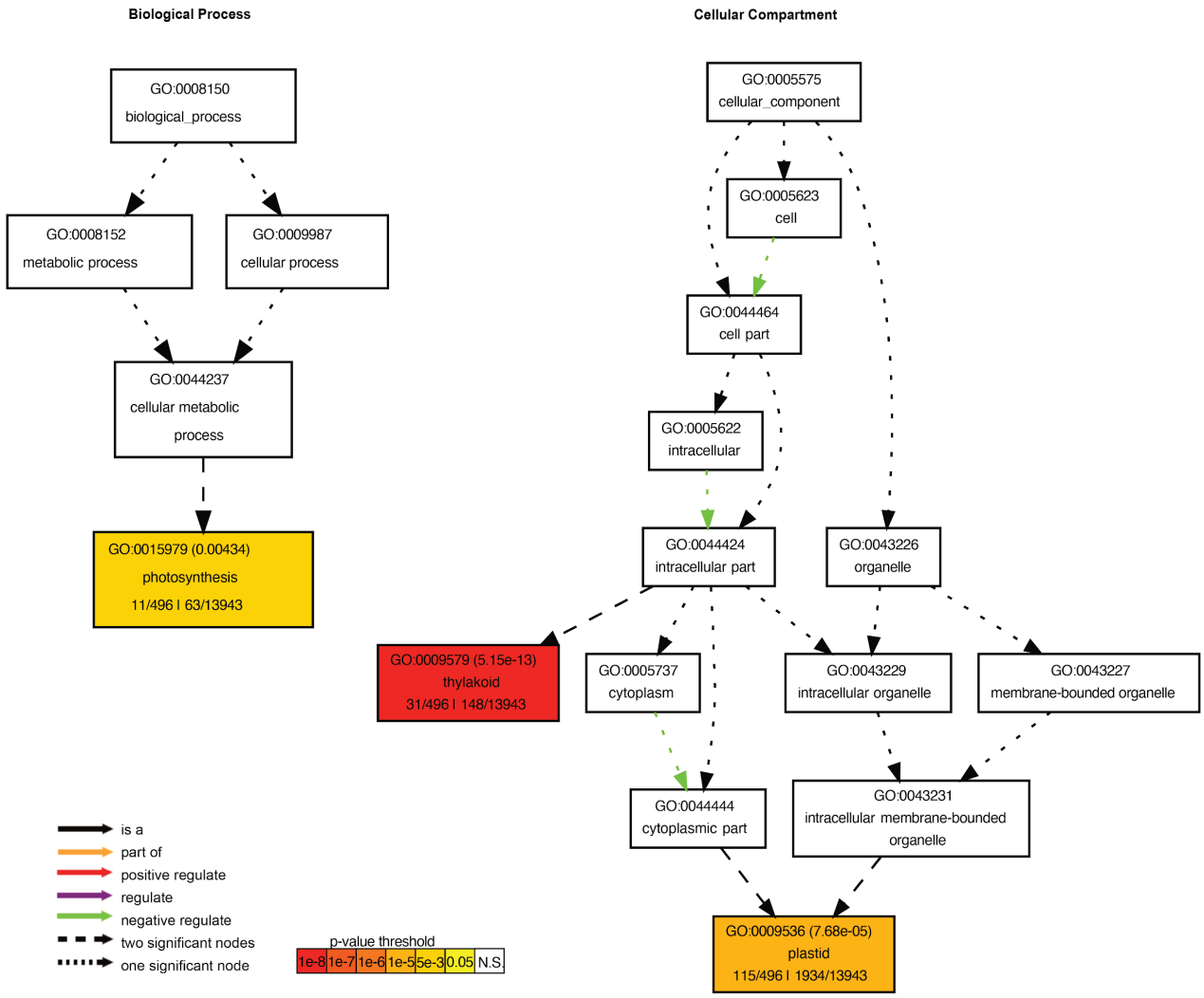

Figure S10. Positive genes are enriched for genes encoding thykaloid-localized proteins that are involved in photosynthetic process. Fisher's Exact Test was used against the background list of filtered expressed genes in SHB2 dataset, using plant GOslim based on TAIR10 annotation.

Rank	Motif	Name	P-value	% Target	No. Target	% Bkgd	No. Bkgd
1		PCF	1e-42	26.65	599	15.27	7252
2		c-Myc	1e-21	19.26	433	12.13	5761
3		BZR	1e-21	16.55	372	9.99	4743

Figure S11. Top 3 motif enrichment results for All-BTH negative genes. All-BTH negative genes are all genes showing negative correlations between dominance of expression with dominance in F1 rosette size when treated with BTH). No.Target: number of genes from All-BTH negative gene list carrying target motif in *cis*, No.Bkgd: number of genes from background gene list carrying target motif in *cis*.

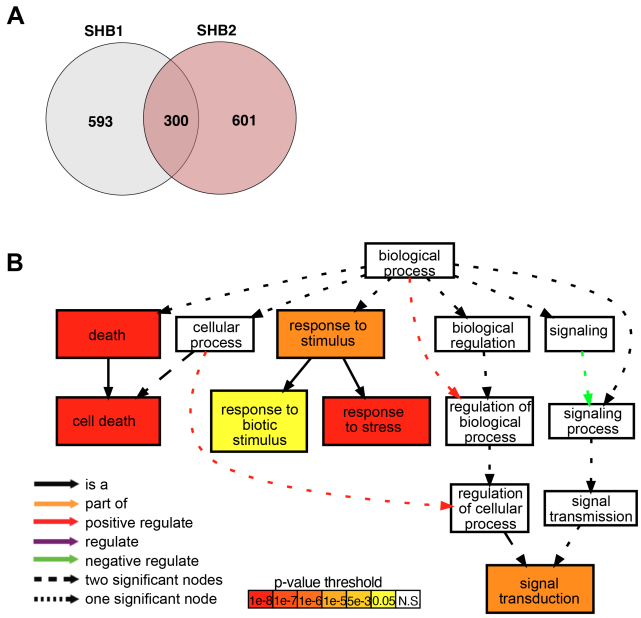

753

754 **Figure S12. Common additive genes.** A. Venn diagram showing the overlapping of additive genes in SHB1

755 and SHB2 experiments. B. GO-term enrichment diagram of common additive genes.

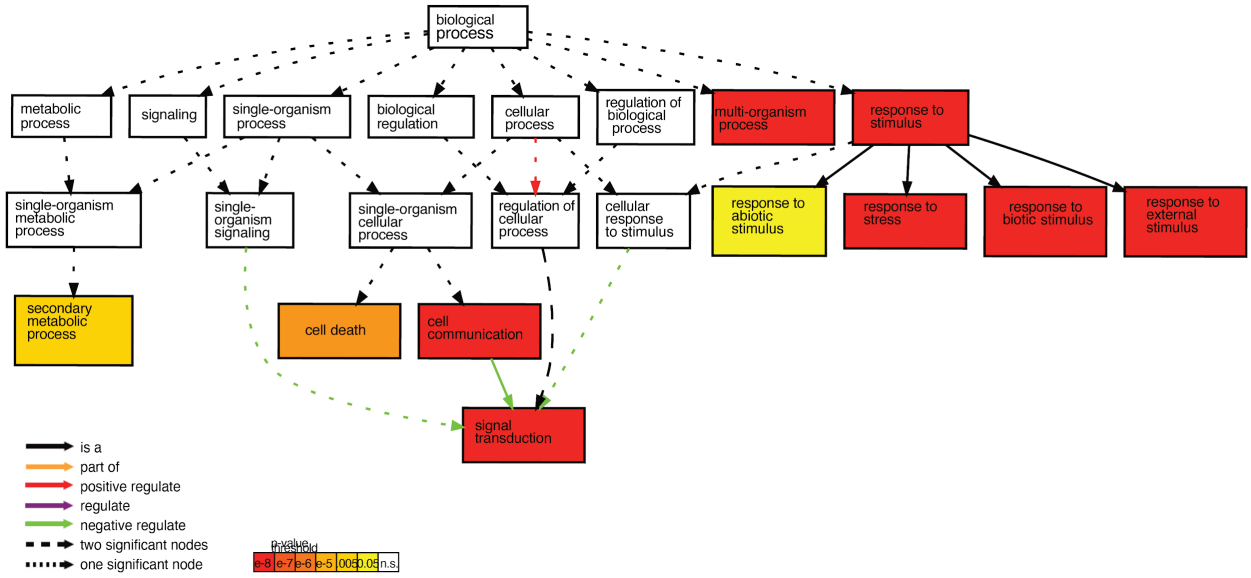

Figure S13. Additive genes in SHB2. This gene set (n=901) is enriched for GO terms of response to stress and (biotic) stimuli, cell death, and secondary metabolic process.

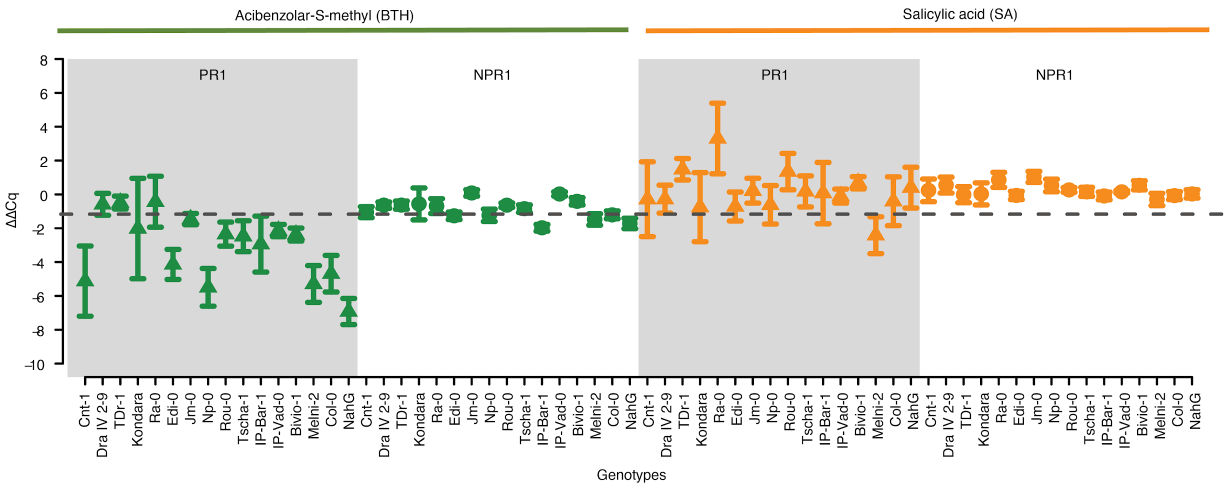

759

760 **Fig. S14. Efficient induction of defense responses in *A. thaliana* accessions with the BTH dosage used.** qRT-
761 PCR of two defense marker genes, *PR1* and *NPR1*, in 16 inbred accessions after BTH and SA treatment. Each
762 dot represents the mean ΔΔCq value against housekeeping genes in mock-treated plants, with error bars
763 indicating the standard deviation of the biological replicates.